Elsevier Editorial System(tm) for Medical Engineering & Physics
Manuscript Draft

Manuscript Number: MEP-D-17-00459R1

Title: Biomechanical Analysis of Bone Remodeling Following Mandibular Reconstruction using Fibula Free Flap

Article Type: Paper

Section/Category: Regular Issue Paper

Keywords: Fibula free flap; Finite element analysis; Jaw biomechanics; Mandibular reconstruction; Bone remodeling.

Corresponding Author: Dr. Nobuhiro Yoda,

Corresponding Author's Institution: Tohoku University Graduate School of Dentistry

First Author: Nobuhiro Yoda

Order of Authors: Nobuhiro Yoda; Keke Zheng; Junning Chen; Zhipeng Liao; Shigeto Koyama; Christopher Peck; Michael Swain; Keiichi Sasaki; Qing Li

Abstract: Whilst the newly established biomechanical conditions following mandibular reconstruction using fibula free flap can be a critical determinant for achieving favorable bone union, little has been known about their association in a time-dependent fashion. This study evaluated the bone healing/remodeling activity in reconstructed mandible and its influence on jaw biomechanics using CT data, and further quantified their correlation with mechanobiological responses through an in-silico approach. A 66-year-old male patient received mandibular reconstruction was studied. Post-operative CT scans were taken at 0, 4, 16 and 28 months. Longitudinal change of bone morphologies and mineral densities were measured at three bone union interfaces (two between the fibula and mandibular bones and one between the osteotomized fibulas) to investigate bone healing/remodeling events. Three-dimensional finite element models were created to quantify mechanobiological responses in the bone at these different time points. Bone mineral density increased rapidly along the bone interfaces over the first four months. Cortical bridging formed at the osteotomized interface earlier than the other two interfaces with larger shape discrepancy between fibula and mandibular bones. Bone morphology significantly affected mechanobiological responses in the osteotomized region ($R2>0.77$). The anatomic position and shape discrepancy at bone union affected the bone healing/remodeling process.

東北大學大学院歯学研究科
Tohoku University Graduate School of Dentistry
4-1 Seiryo-machi, Aoba-ku, Sendai 980-8575 Japan

**Dr. Nobuhiro Yoda**
*Assistant Professor*

Division of Advanced Prosthetic Dentistry, Tohoku University Graduate School of Tohoku University Graduate School of Dentistry
4-1 Seiryo-machi, Aoba-ku, Sendai 980-8575, JAPAN
Telephone: +81-22-717-8369
Facsimile: +81-22-717-8371
Email: nobuhiro.yoda.e2@tohoku.ac.jp

24 February 2018

Dr Richard A Black, Editor-in-Chief
*Medical Engineering & Physics*

Dear Dr Black,

First of all, we would like to take this chance to thank you for your kind consideration and editorial review of our paper. The editors and the reviewers indeed provided us with highly constructive comments and suggestions, which I believe helped us to make our paper in a much better quality.

Please find the revision of the manuscript and detailed point-by-point responses. We have carefully considered all the comments raised and seriously revised the paper. After many discussion sessions now we all agree to submit you our revision for your further consideration.

Thank you very much again for your consideration of the paper. We look forward to hearing from you at your earliest convenience.

Yours sincerely,

Nobuhiro Yoda

Nobuhiro Yoda, DDS, PhD

# Declaration

The authors affirm that this manuscript, entitled "Biomechanical Analysis of Bone Remodeling Following Mandibular Reconstruction using Fibula Free Flap" has been submitted solely to *Medical Engineering & Physics* and that it is not concurrently under consideration for publication in another journal.

The authors also confirm that the submitted work, including images, are original and there is no conflict of interest in this submitted work.

| **Authors** | **Signatures** |
|---|---|
| Nobuhiro Yoda | |
| Keke Zheng | |
| Junning Chen | |
| Zhipeng Liao | |
| Shigeto Koyama | |
| Christpher Peck | |
| Keiichi Sasaki | |
| Michael V. Swain | |
| Qing Li | |

**Author Contributions**

(1) the conception and design of the study, or acquisition of data, or analysis and interpretation of data: NY KZ SK KS MS QL.

(2) drafting the article or revising it critically for important intellectual content: NY KZ JC ZL CP KS MS QL.

(3) final approval of the version to be submitted: NY KZ JC ZL SK CP KS MS QL.

Manuscript Number MEP-D-17-00459

**Point-by-point responses to the reviewers' comments on the manuscript**

**Article Title: Biomechanical Analysis of Bone Remodeling Following Mandibular Reconstruction using Fibula Free Flap**

Dear Editors and Reviewers,

We wish to thank you and expert reviewers for providing the very constructive comments and insightful suggestions on our manuscript. They have helped greatly enhance our manuscript. By closely following your suggestions and incorporating extra information, we hope that the revised manuscript meets the standard of publication for *Medical Engineering & Physics*.

We hope our dedicated revision have addressed all of your concerns. A detailed point-by-point response is provided as follows.

We look forward to hearing from you again at your earliest convenience.

Yours sincerely,

Nobuhiro Yoda, DDS, PhD.

東北大學大学院歯学研究科
Tohoku University Graduate School of Dentistry
4-1 Seiryo-machi, Aoba-ku, Sendai 980-8575 Japan

Biomechanical Analysis of Bone Remodeling Following Mandibular Reconstruction using Fibula Free Flap

## Highlights

- The longitudinal changes in bone morphology and mineral density systematically in the course of healing/remodeling after mandibular reconstruction with fibula free flap were quantified;
- The mutual influence between the changes in tissue conditions and mandibular mechanobiology by establishing a combined *in-vivo* and *in-silico* approach was assessed for the first time;
- Novel understanding of mechanobiological responses in a healing and remodeling of mandible following mandibular reconstruction was provided.

*Manuscript - clean copy

# Biomechanical Analysis of Bone Remodeling Following Mandibular Reconstruction using Fibula Free Flap

Nobuhiro Yoda*[1,2], Keke Zheng[2], Junning Chen[3], Zhipeng Liao[2], Shigeto Koyama[4], Christopher Peck[5], Michael Swain[6], Keiichi Sasaki[1], and Qing Li[2].

[1]Division of Advanced Prosthetic Dentistry, Tohoku University Graduate School of Dentistry, 4-1, Seiryo-machi, Aoba-ku, Sendai, Miyagi, 9808575, Japan

[2]School of Aerospace, Mechanical and Mechatronic Engineering, The University of Sydney, NSW 2006, Australia

[3]Department of Biomaterials, Max Planck Institute of Colloids and Interfaces, Am Mühlenberg 1 OT Golm, 14476 Potsdam, Germany

[4]Maxillofacial Prosthetics Clinic, Tohoku University Hospital, 1-1, Seiryo-machi, Aoba-ku, Sendai, Miyagi, 9808575, Japan

[5]Faculty of Dentistry, The University of Sydney, Sydney, NSW, 2006, Australia

[6]Department of Bioclinical Sciences, Faculty of Dentistry, Kuwait University, Safat 13110, Kuwait

*** Corresponding Author: Nobuhiro Yoda**

**Contact details:**

Address: Division of Advanced Prosthetic Dentistry, Tohoku University Graduate School of Dentistry, 4-1, Seiryo-machi, Aoba-ku, Sendai, Miyagi, 9808575, JAPAN

Phone: +81-22-717-8369; Fax: +81-22-717-8371;

E-mail: nobuhiro.yoda.e2@tohoku.ac.jp

# Abstract

Whilst the newly established biomechanical conditions following mandibular reconstruction using fibula free flap can be a critical determinant for achieving favorable bone union, little has been known about their association in a time-dependent fashion. This study evaluated the bone healing/remodeling activity in reconstructed mandible and its influence on jaw biomechanics using CT data, and further quantified their correlation with mechanobiological responses through an *in-silico* approach. A 66-year-old male patient received mandibular reconstruction was studied. Post-operative CT scans were taken at 0, 4, 16 and 28 months. Longitudinal change of bone morphologies and mineral densities were measured at three bone union interfaces (two between the fibula and mandibular bones and one between the osteotomized fibulas) to investigate bone healing/remodeling events. Three-dimensional finite element models were created to quantify mechanobiological responses in the bone at these different time points. Bone mineral density increased rapidly along the bone interfaces over the first four months. Cortical bridging formed at the osteotomized interface earlier than the other two interfaces with larger shape discrepancy between fibula and mandibular bones. Bone morphology significantly affected mechanobiological responses in the osteotomized region ($R^2$>0.77). The anatomic position and shape discrepancy at bone union affected the bone healing/remodeling process.

**Keywords:** Fibula free flap; Finite element analysis; Jaw biomechanics; Mandibular reconstruction; Bone remodeling.

# 1. Introduction

Free vascularized osteocutaneous tissue transfer has become a well-established procedure for maxillomandibular reconstruction following large resection due to trauma, atrophy, and tumors ablation [1,2]. Fibula free flap (FFF) provides superior length and long vascular pedicles for mandibular reconstruction, with proven subsequent high reliability and adaptability [3]. Nevertheless, some clinical complications remain with delayed or poor union between the grafted fibula bone and host native mandible [4,5]. Recent CT evaluations reported 20% [6] and 9% [7] non-union rates, respectively. Bone union determines the strength and health of the reconstructed mandible, both of which are essential for further occlusal and prosthetic rehabilitation. In the case of bone fracture healing, the mechanobiological environment, which is thought to regulate cellular behaviors, can be a critical determinant [8].

Unlike general bone fracture healing processes, FFF mandibular reconstruction may be affected by additional factors, such as shape discrepancy between different bones and poor bone vascularity [4,9]. Further, the loss of several masticatory muscles due to resection can cause unbalanced jaw movement and abnormal mastication, leading to significant change in the biomechanical conditions [10,11]. Thus the mechanobiological responses in the jaw can be altered significantly; and such a change in-turn affects subsequent bone remodeling activities [12,13]. To assist surgical planning and oral rehabilitation it is essential to understand bone healing/remodeling activity and its influence on jaw biomechanics, thereby preventing delayed or poor union of bone grafts.

Finite element (FE) analysis has the adequacy for the biomechanical studies on orthopaedic [14-16] and dental problems [17-19]. Several those studies demonstrated their compelling advantages for understanding the biomechanics and mechanobiology of reconstructed mandibles *in-silico* [20,21]. With recent advances in micro computerized tomography (CT), bone mineral density (BMD) and morphological changes can be measured to evaluate bone remodeling sequences noninvasively [13,22,23]. The CT-based 3D FE models can be thus created to quantify biomechanical responses to functional forces in a patient-specific and time-dependent manner [24,25].

This study aims to (1) examine longitudinal changes in bone morphology and mineral density in the course of healing/remodeling after mandibular reconstruction with FFF; and (2) investigate the associated variation in mandibular biomechanics in terms of mechanical stimulus. The postoperative CT scans were performed at 4 critical time points over two and half years' clinical follow-up, and the CT images were segmented for both 2D multiple planar reconstructions (MPR) and 3D (volumetric) analyses. The bone condition was analyzed in both spatial and temporal manner, in terms of morphology and BMD. Nonlinear 3D FE analyses were conducted to quantify the bone mechanobiological stimuli at these different time points; and then correlated to the corresponding *in-vivo* clinical data. By establishing this combined *in-vivo* and *in-silico* approach, the mutual influence between tissue conditions and mandibular mechanobiology was assessed. The results are expected to provide important insights into surgical plan for mandibular reconstruction.

# 2. Materials and Methods

### *2.1 Clinical Treatment*

A 66-year-old male patient received mandibular reconstruction with osteotomized FFF, due to a squamous-cell carcinoma at the right molar gingiva at the Department of Otolaryngology-Head and Neck Surgery, Tohoku University Hospital in Japan. Upon harvesting, the fibular bone was segmented to match the defect jaw morphology. A titanium fixation plate (Synthes, Solothurn, Switzerland), which was pre-bent using the CT-based 3D patient model before surgery, was configured to be fixed monocortically with a total of 11 titanium screws (Synthes, Solothurn, Switzerland) as shown in Fig. 1. The first CT scan (M0) was performed at the end of surgery, and the follow-up CTs were taken at 4, 16 and 28 months after surgery (namely, M4, M16, and M28, respectively). A removable partial denture was inserted into this subject 6 months after the surgery; however, the subject did not use it for mastication, due to fear of biting on the reconstructed side. The periodontal conditions of the remaining teeth and the removable partial denture have been maintained at the Maxillofacial Prosthetics Clinic in Tohoku University Hospital every three months.

### *2.2 CT Imaging Acquisition and 2D Image Analysis*

Multi-detector helical CT scans were performed for the follow-up examinations using Somatom Emotion 6 (Siemens, Erlangen, Germany) at 120 kV and 80 mA with the spatial resolution of 0.4, 0.4, and 0.8 mm in the radial, tangential, and axial directions. The CT data was further processed with the medical image viewer software (EV Insite S, PSP Co., Tokyo, Japan), for the detection and alignment of anatomic landmarks between the different cross-sectional examinations. The mandibular plane was defined using three reference points; namely, left Gonion point, Menton point, and inflection point of a titanium fixation plate (green triangles in Fig. 2a). Six planes parallel to this mandibular plane were selected for the quantitative analysis of bone union at three docking sites (DS1, DS2, and DS3, respectively) with 2 mm intervals by multiple planar reconstructions (MPR) (Fig. 2b) [12]. On each plane, a 2 $mm^3$ volume of interest (VOI) was considered along the superior-inferior axis (Fig. 2b). Since a significant correlation between Hounsfield units (HU) obtained from clinical CT scans and bone mineral density (BMD) were established [26], the HU values change in VOIs can be regarded as the BMD changes over time here, particularly for bone unification at the contact interfaces. All the VOIs were placed at the same positions throughout these four time points, based on the distance from the titanium fixation plate and screws as a reference.

### *2.3 3D Registration and Volumetric Analysis*

3D registration was carried out for investigating the longitudinal changes in bone surface profile and mineral density using Amira 2016.22 (Zuse Institute Berlin (ZIB), Berlin, Germany) (Fig. 3a). The titanium fixation plate was selected as the reference geometry for its rigidness and high contrast. To quantify the variation of BMD at the docking sites, the change in greyscales was correlated with the distance from the inferior to the superior aspect. The average value of the pixel intensity (i.e. greyscale) was calculated in the cortical bone region on each slice (at a regular spacing of 0.8 mm along the coronal axis), enabling a plot of pixel value change along the axial direction. To determine the HU values of the cortical bone, several profile lines were constructed at the CT images cross the region of mature cortical bone. By sampling the histogram distribution, a HU value of 1536 was determined to be a threshold for determining cortical bone pixels, which is consistent with the reported HU value of cortical bone for cone beam CT in literature [27]. By using this cortical bone threshold, variation in both bone density and volume at the same region for the four time points were quantified. The detailed variation in bone volume (i.e. volume of the cortical bone voxel cuboids) along this direction was plotted using the same approach. In addition, the variation in pixel number, rather than the pixel intensity, in the cortical bone region was considered.

### *2.4 Finite Element Analysis*

Four case-specific FE models were created based on the CT data taken at M0, M4, M16, and M28, respectively [28,29]. The CT images were imported into ScanIP Ver. 4.3 (Simpleware Ltd, Exeter, UK) for segmentation. The segmented masks (bone, individual tooth and titanium fixation plate) were further processed in Rhinoceros 4.0 (Robert McNeel & Associates, Seattle, USA) to create parametric models with non-uniform rational B-spline (NURBS) (Fig. 3b). Following the development of the mandibular models, the total 11 fixation screws were modeled according to the manufacturing specifications in Solidworks 2013 (SolidWorks Corp, Waltham, MA, USA). Those screws were virtually inserted into the models in Rhinoceros 4.0 as guided by the CT images. Considering that the patient disuse the denture in his daily life and has no parafunctional habit, the denture was not inserted in the models. To ensure the numerical accuracy, an adaptive mesh was generated based on a mesh convergence test. Ten-node quadratic tetrahedral elements with hybrid formulation (C3D10H) were adopted to ensure smoothness along the contact interfaces.

A pixel-based mapping algorithm was adopted to create the heterogeneous bone density distributions at the different time points, reflecting the changes of the anatomical conditions [29]. A homogeneous isotropic linear-elastic model was used to define the teeth (Young's modulus $E = 20{,}000$ MPa, Poisson's ratio $\nu = 0.2$), titanium fixation plates and screws (Ti6Al7Nb: $E=110{,}000$ MPa, $\nu=0.3$) [21,30].

The hinge constraints were prescribed for the corresponding mandibular condyles. In this subject, the large bone resection was accompanied by the functional loss of the right masseter, medial pterygoid and temporalis muscles; and consequently masticatory conditions changed dramatically post-surgery. Due to lack of information regarding muscular forces after such a large resection [20], the magnitudes and directions of individual forces were derived based on the literature for the remaining muscles (masseter mascle: 59.23 N, medial pterygoid muscle: 39.60 N, lateral pterygoid muscle: 34.44 N, and temporalis: 34.09 N, respectively) [31].

Strain energy density (SED) was quantified as a mechanobiological stimulus to analyze the bone responses in the three docking sites and VOIs. SED has been considered an effective stimulus to bone remodeling in long bones [32] and mandible [24,33] and can be a scalar quantity to combine stress and strain but eliminate their directionalities [34]. The SEDs at different time points were correlated with the corresponding change in the bone density. In this study, linear regression analysis was performed using IBM SPSS Statistics Ver. 21.0 (IBM Corp., New York, NY, USA) to examine the correlations between stimuli and bone remodeling progression in all VOIs. The $R^2$ values presented the goodness of fit for the predictor functions, thereby indicating the extent of correlation.

# 3. Results

### *3.1 MPR Image Assessment for Bone Morphology and Mineral Density*

Fig. 4 shows the longitudinal changes in bone profile from the CT-based MPR images. In docking site DS1, a significant amount of callus bone formed at time point M4, and the cortical bridging successfully formed in both buccal and lingual regions at M16. In DS2, the cortical bridging formed at M4 in both the buccal and lingual regions. Also, the cortical-like bone appeared to fill the entire interface, while some resorption occurred at the upper and bottom surfaces of cortical bone. In DS3, there was large discrepancy of bone shape at the initial stage. However, the bone shapes gradually remodeled and cortical bridging was found in both the buccal and lingual regions at M16.

Fig. 5 shows that the averaged HU value was calculated for each VOI to quantify the change of BMD. For DS1, both superior and inferior cortical bones underwent resorption from M0 to M16, while the BMD peaked in the trabecular interface regions at M4 before undergoing resorption. In contrast, the grafted bones at DS2 performed exceedingly well in terms of new bone formation, despite being osteotomized, seen in rapid increases of BMD in the first four months. For DS3, the cancellous/trabecular region underwent much more dramatic remodeling than the cortical bone with rapid increase in BMD from M0 to M4 but decrease from M4 to M16.

### *3.2 Volumetric Assessment of Bone Mineral Density and Morphology*

Bone morphological changes were visualized as the apposition and resorption on the bone surface by 3D volumetric registration in the three docking sites (Fig. 6). The longitudinal changes in bone volume were site-specific and the rate of volume increase in the cortical bone region was positive in all the three sites from M4 to M16 (Fig. 7a). Fig. 7b exhibits the longitudinal change rate of bone volume at each docking site. Bone volume increased remarkably from M4 to M16 due to new bone formation, especially at the region from 15 mm to 25 mm for DS1 and from 20 mm to 30 mm for DS3 on the sectional plane of mandible as visualized in Fig. 6. Fig. 7c plotted the site-specific change rate of BMD based on the average grayscale in the cortical bone region. Note that the BMD decreased in the first four months for all the docking sites.

### *3.3 Mechanobiological Stimulus Distribution*

Fig. 8 shows the longitudinal changes in the SED distribution and corresponding CT MPR images of the reconstructed mandible. Both global and local SED distributions changed with time significantly. The longitudinal changes in morphology and BMD were remarkable particularly for DS1, leading to substantial variation in the SED distribution.

The SED at VOIs in the cortical bone region was generally higher than that in the cancellous region in DS1 and DS2 (Fig. 9). At each VOI, the SED decreased with time at DS1 and DS3, especially in the superior region of DS1. While the increase in SED with time could be found in some VOIs, the SED dropped from M0 to M4 and then gradually increased till M28 (but never exceeds that at M0), at 6, 8, and 10 mm VOIs in DS2.

Linear regression analysis between the HU values and SED in VOIs indicated that there was a strong dependence on the HU values only in DS2 ($p<0.05$), as shown in Fig. 10.

# 4. Discussion

Both 2D MPR images and 3D volumetric analyses enabled to quantify and visualize time-dependent bone apposition and resorption in terms of morphology and BMD in this FFF reconstructive mandible. This study is believed to be the first of its kind for investigating the anatomical sequence of healing/remodeling process and its correlation with mechanobiological responses in a reconstructive mandible.

The clinical process of cortical bridging at bone docking regions was found to be significantly site-specific based on the results of both 2D MPR images and 3D volumetric analyses. Biological healing at bone union is influenced by complex cellular and molecular activities, and can be affected by the dimension of bone segment gap [35] and contact shape [9]. In this study, we set up a criterion to justify the cortical bridging, namely, no gap was observed between the two bones in the six cross sectional planes as shown in Fig. 4. According to this criterion, the contact region in DS2 achieved earlier cortical bridging than the other two sites.

The BMD became higher within the first four months in all the VOIs except for the cortical bone regions in DS1 (Fig. 5). Those cortical regions appeared to undergo significant resorption, while the osseous callus was generally found at the interface of trabecular regions during the bone-healing phase [36,37]. The BMDs of all the cortical bone regions in the docking sites were also found to decrease in the first four months, which was most remarkable for DS2 (Fig. 7c). Despite a vascularized bone graft, the lower bone vascularity may have caused the reduction of BMD on the cortical region of the fibula graft [38,39]. Despite the lowered BMD, 3D volumetric analysis revealed a higher increase rate of bone volume in DS1 than the other two sites over the same time period (Fig. 7a). Primary bone apposition may have developed throughout formation of the osseous callus at the endochondral and periosteal areas (Figs. 4 and 5) [35]. The woven bone with low BMD appears to initially form for filling the gap and reducing morphological discrepancy, which may be related to the initial volume increase in DS1. Lamellae bone with high BMD appears to form after M4 [37]. Lower bone vascularity in the distal segment of osteotomy [39] may limit those biological healing activities in DS2 and DS3 compared to DS1, further contributing to the initial reduction in the bone volume (Fig. 7a).

Considering the positive increase rates attributable to bone apposition at all three docking sites from M4 to M16, bone (re)modeling activity had a primary effect on post-healing bone formation [40,41]. Osseous callus at the interface regions in DS1 and DS3 gradually became cancellous bone, forming a natural mandibular structure during the course. Nevertheless, the healing and remodeling process at the docking site, especially with large shape discrepancy, is considered to be significantly slower than those of the general bone fracture [37,42]. Note that the mandible can be distorted during daily oral function [43]. Despite the mechanical fixation by titanium plate, the distortion can affect the mechanical stability of the docking sites, which might also delay the healing process [9].

Mechanical loading is known to stimulate bone healing and remodeling process, likely enhancing bone mass and functionality [40]. The mechanobiological impetus can thus be related to the bone remodeling activity [12,13]. SED has been considered an effective stimulus to bone remodeling in long bones [32] as well as mandible [24,33]. This study revealed the correlation between SED and healing/remodeling outcome over the time period concerned.

The variation in SED distribution was attributed to the time longitudinal change in the mandibular morphology (Figs. 8 and 9), as well as load transfer in the restructured mandible, particularly through the fibula grafts. In other words, the functional load was initially transferred to the fibula graft completely via the titanium fixation plate (M0); but subsequently, a greater proportion of load transferred through the bony tissue as the extent of bone union increased. In addition, the remaining unbalanced muscle activities readapt with time [10,11]. All these factors have a collective effect on the mechanobiological responses.

As shown in Fig. 10, the SED had a strong dependence on the HU values in DS2 ($p<0.05$). The HU value altered the load bearing capability of the fibula bone, meaning that the SED is associated with HU values. Lower bone vascularity and good bone contact condition at DS2 possibly enhance the effect of mechanobiological stimuli on BMD adaptation, which might be related to the earlier process of cortical bridging at the DS2. For DS1 and DS3, significant shape discrepancy due to reconstruction generated non-physiological stress/strain concentration, which might have distorted the distribution of SED and its correlation to remodeling.

Clinically, the implant-supported denture is considered as the most suitable option for functional rehabilitation following mandibular reconstruction [2]. Although the timing of implant placement is still controversial, several studies adopted the time for implant placement at least 6-12 months after the reconstruction with FFF [1,44,45]. Considering the cortical bridging as a predictor of bone union strength [7,46], all the bone unions can be confirmed through CT scanning, especially in the cases with a large bone discrepancy. Specifically, favorable initial bone contacts with small shape discrepancy are considered a primary factor for earlier success of cortical bridging.

There are still some limitations in this study. Constrained by the clinical protocol and radiation dosage allowance, the scanning resolution of CTs could have affected modeling accuracy. The FE analyses still included several assumptions, such as simulation under static loading conditions and rotational movement on the mandibular condyles. The applied muscle forces did not precisely reflect specific condition of this subject; plus the muscle forces are anticipated to change over time after reconstruction [47,48]. Consequently, the resultant reaction responses on both temporomandibular joints might become asymmetric and physiologically complicated. Finally, while the study was featured as patient-specific, the results were based on only one particular subject. In addition, other patient's factors, such as the systematic background and the treatment process, could be generally the decisive factors to the bone healing and remodeling process at the docking sites. Further evaluation and data acquisition of other subjects with inevitably varied conditions are necessary before generalizing these clinical and biomechanical findings.

## 5. Conclusion

This newly developed analysis procedure provided a quantitative clinical follow-up of mandibular reconstruction with fibula free flap (FFF) and fundamental understanding of time-dependent biomechanical responses in the reconstructed mandible. It was found that the bone healing and remodeling process at the docking sites were site-specific; and cortical bridging in the osteotomized region took place faster than that in the other docking sites between mandibular and fibula bones for the specific patient concerned. Within the limitation of this study, the anatomic position and the discrepancy of initial shape at the docking sites between the host mandible and fibula graft affected the bone healing and remodeling process. It divulged a correlation between mechanobiological stimulus (strain energy density - SED) and the longitudinal change in bone mineral density (BMD) and morphology, especially at the osteotomized region. The longitudinal CT data and mechanobiological correlation generated in this study provided new insights into patient-specific surgical planning and occlusal rehabilitation.

## Conflict of interests

None declared.

## Ethical approval

The research protocol was approved by the research ethics committee of the Tohoku University Graduate School of Dentistry (reference #24-10). Full written informed consent was obtained to use the CT images for this study. All procedures performed in this study were in accordance with the ethical standards of the 1964 Helsinki Declaration (http://www.wma.net) and its later amendments.


## Acknowledgements

This work was supported by the Australian Research Council (ARC) through the Discovery and Fellowship schemes (DP160104602 and FT120100947). We are grateful to Dr. Atsushi Takeda and Dr. Naoko Sato at Tohoku University Hospital for providing and caring for this study patient.

# References

[1] Hakim SG, Kimmerle H, Trenkle T, Sieg P, Jacobsen HC. Masticatory rehabilitation following upper and lower jaw reconstruction using vascularised free fibula flap and enossal implants-19 years of experience with a comprehensive concept. Clin Oral Invest 2015; 19: 525-34.

[2] Chiapasco M, Biglioli F, Autelitano L, Romeo E, Brusati R. Clinical outcome of dental implants placed in fibula-free flaps used for the reconstruction of maxillo-mandibular defects following ablation for tumors or osteoradionecrosis. Clin Oral Implants Res 2006; 17: 220-28.

[3] Hidalgo DA, Rekow AA. Review of 60 consecutive fibula free flap mandible reconstructions. Plast Reconstr Surg 1995; 96: 585-96.

[4] Virgin FW, Iseli TA, Iseli CE, Sunde J, Carroll WR, Magnuson JS, Rosenthal EL. Functional outcomes of fibula and osteocutaneous forearm free flap reconstruction for segmental mandibular defects. Laryngoscope 2010; 120: 663-7.

[5] Nam W, Kim HJ, Choi EC, Kim MK, Lee EW, Cha IH. Contributing factors to mandibulotomy complications: A retrospective study. Oral Surg Oral Med Oral Pathol Oral Radio Endod 2006; 101: e65-70.

[6] Yla-Kotola TM, Bartlett E, Goldstein DP, Armstrong K, Gilbert RW, Hofer SOP. Union and bone resorption of free fibular flaps in mandibular reconstruction. J Reconstr Microsurg 2013; 29: 427-32.

[7] Akashi M, Hashikawa K, Kakei Y, Sakakibara A, Hasegawa T, Minamikawa T, Komori T. Sequential evaluation for bone union of transferred fibula flaps in

reconstructed mandibles: Panoramic x-ray versus computed tomography. Int J Oral Maxillofac Surg 2015; 44: 942-7.

[8] Gerstenfeld LC, Cullinane DM, Barnes GL, Graves DT, Einhorn TA. Fracture healing as a post-natal developmental process: Molecular, spatial, and temporal aspects of its regulation. J Cell Biochem 2003; 88: 873-84.

[9] Feron JM, Mauprivez R. Fracture repair: General aspects and influence of osteoporosis and anti-osteoporosis treatment. Injury 2016; 47 Suppl: 10-4.

[10] Hannam AG, Stavness IK, Lloyd JE, Fels SS, Miller AJ, Curtis DA. A comparison of simulated jaw dynamics in models of segmental mandibular resection versus resection with alloplastic reconstruction. J Prosthet Dent 2010; 104: 191-8.

[11] Namaki S, Morimoto M, Ohba H, Tanaka H, Koshikawa N, Shinohara M. Masticatory efficiency before and after surgery in oral cancer patients: Comparative study of glossectomy, marginal mandibulectomy and segmental mandibulectomy. J Oral Sci 2004; 46: 113-7.

[12] Suenaga H, Chen J, Yamaguchi K, Li W, Sasaki K, Swain M, Li Q. Mechanobiological bone reaction quantified by positron emission tomography. J Dent Res 2015; 94: 738-44.

[13] Chen J, Ahmad R, Suenaga H, Li W, Swain M, Li Q. A comparative study on complete and implant retained denture treatments - a biomechanics perspective. J Biomech 2015; 48: 512-9.

[14] Mercuri EGF, Daniel AL, Hecke MB, Carvalho L. Influence of different

mechanical stimuli in a multi-scale mechanobiological isotropic model for bone remodelling. Med Eng Phys 2016; 38: 904-10.

[15] Yamako G, Chosa E, Zhao X, Totoribe K, Watanabe S, Sakamoto T, Nakane N. Load-transfer analysis after insertion of cementless anatomical femoral stem using pre- and post-operative CT images based patient-specific finite element analysis. Med Eng Phys 2016; 36: 694-700.

[16] Zheng K, Scholes C, Chen J, Parker D, Li Q. Multiobjective optimization of cartilage stress for non-invasive, patient-specific recommendations of high tibial osteotomy correction angle. Med Eng Phys 2017; 42: 26-34.

[17] Odin G, Savoldelli C, Bouchard PO, Tillier Y. Determination of Young's modulus of mandibular bone using inverse analysis. Med Eng Phys 2010; 32: 630-37.

[18] Bonnet AS, Postaire M, Lipinski P. Biomechanical study of mandible bone supporting a four-implant retained bridge Finite element analysis of the influence of bone anisotropy and foodstuff position. Med Eng Phys 2009; 31: 806-15.

[19] Haiat G, Wang HL, Brunski J. Effects of biomechanical properties of the bone-implant interface on dental implant stability: from in silico approaches to the patient's mouth. Annu Rev Biomed Eng 2014; 16: 187-213.

[20] Narra N, Valasek J, Hannula M, Marcian P, Sandor GK, Hyttinen J, Wolff J. Finite element analysis of customized reconstruction plates for mandibular continuity defect therapy. J Biomech 2014; 47: 264-8.

[21] Tie Y, Wang DM, Ji T, Wang CT, Zhang CP. Three-dimensional finite-element

analysis investigating the biomechanical effects of human mandibular reconstruction with autogenous bone grafts. J Craniomaxillofac Surg 2006; 34: 290-8.

[22] Birkhold AI, Razi H, Weinkamer R, Duda GN, Checa S, Willie BM: Monitoring in vivo (re)modeling: A computational approach using 4d microct data to quantify bone surface movements. Bone 2015; 75: 210-21.

[23] Lukas C, Ruffoni D, Lambers FM, Schulte FA, Kuhn G, Kollmannsberger P, Weinkamer R, Muller R. Mineralization kinetics in murine trabecular bone quantified by time-lapsed in vivo micro-computed tomography. Bone 2013; 56: 55-60.

[24] Rungsiyakull C, Chen J, Rungsiyakull P, Li W, Swain M, Li Q. Bone's responses to different designs of implant-supported fixed partial dentures. Biomech Model Mechanobiol 2015; 14: 403-11.

[25] C Field, Q Li, W Li, M Thompson, M Swain. Prediction of mandibular bone remodelling induced by fixed partial dentures. J Biomech 2010; 43: 1771-9.

[26] Schreiber JJ, Anderson PA, Rosas HG, Buchholz AL, Au AG. Hounsfield units for assessing bone mineral density and strength: A tool for osteoporosis management. J Bone Joint Surg 2011; 93a: 1057-63.

[27] Reeves TE, Mah P, McDavid WD. Deriving hounsfield units using grey levels in cone beam CT: a clinical application. Dentomaxillofac Radiol 2012; 41: 500-8.

[28] Yoda N, Liao Z, Chen J, Sasaki K, Swain M, Li Q. Role of implant configurations supporting three-unit fixedpartial denture on mandibular bone

response: biological-data-based finite element study. J Oral Rehabil 2016; 43: 692-701.

[29] Liao Z, Chen J, Zhang Z, Li W, Swain M, Li Q. Computational modeling of dynamic behaviors of human teeth. J Biomech 2015; 48: 4214-20.

[30] Chen J, Li W, Swain MV, Ali Darendeliler M, Li Q. A periodontal ligament driven remodeling algorithm for orthodontic tooth movement. J Biomech 2014; 47: 1689-95.

[31] Cruz M, Wassall T, Toledo EM, Barra LP, Lemonge AC. Three-dimensional finite element stress analysis of a cuneiform-geometry implant. Int J Oral Maxillofac Implants 2003; 18: 675-84.

[32] Huiskes R, Ruimerman R, van Lenthe GH, Janssen JD. Effects of mechanical forces on maintenance and adaptation of form in trabecular bone. Nature 2000; 405: 704-6.

[33] Lin D, Li Q, Li W, Duckmanton N, Swain M. Mandibular bone remodeling induced by dental implant. J Biomech 2010; 43: 287-93.

[34] Lin D, Li Q, Li W, Zhou S, Swain MV. Design optimization of functionally graded dental implant for bone remodeling. Composites Part B 2009; 40: 668-75.

[35] Ai-Aql ZS, Alagl AS, Graves DT, Gerstenfeld LC, Einhorn TA. Molecular mechanisms controlling bone formation during fracture healing and distraction osteogenesis. J Dent Res 2008; 87: 107-18.

[36] Vanroermund PM, Romeny BMT, Schoonderwoert GJ, Brandt CJWM, Sijbrandij S, Renooij W. The use of computed-tomography to quantitate bone-

formation after distraction epiphysiolysis in the rabbit. Skeletal Radiol 1987; 16: 52-6.

[37] Yuasa M, Mignemi NA, Barnett JV, Cates JM, Nyman JS, Okawa A, Yoshii T, Schwartz HS, Stutz CM, Schoenecker JG. The temporal and spatial development of vascularity in a healing displaced fracture. Bone 2014; 67: 208-21.

[38] Jacobsen C, Lubbers HT, Obwegeser J, Soltermann A, Gratz KW. Histological evaluation of microsurgical revascularized bone in the intraoral cavity: Does it remain alive? Microsurgery 2011; 31: 98-103.

[39] Chiodo AA, Gur E, Pang CY, Neligan PC, Boyd JB, Binhammer PM, Forrest CR. The vascularized pig fibula bone flap model: Effect of segmental osteotomies and internal fixation on blood flow. Plast Reconstr Surg 2000; 105: 1004-12.

[40] Birkhold AI, Razi H, Duda GN, Weinkamer R, Checa S, Willie BM. The influence of age on adaptive bone formation and bone resorption. Biomaterials 2014; 35: 9290-301.

[41] Christen P, Ito K, Ellouz R, Boutroy S, Sornay-Rendu E, Chapurlat RD, van Rietbergen B. Bone remodelling in humans is load-driven but not lazy. Nat Commun 2014; 5: 4855.

[42] Shirota T, Schmelzeisen R, Ohno K, Michi KI. Experimental reconstruction of mandibular defects with vascularized iliac bone grafts. J Oral Maxillofac Surg 1995; 53: 566-71.

[43] Korioth TWP, Hannam AG. Deformation of the mandible during simulated tooth clenching. J Dent Res 1994; 73: 56-66.

[44] Anne-Gaelle B, Samuel S, Julie B, Renaud L, Pierre B. Dental implant placement after mandibular reconstruction by microvascular free fibula flap: Current knowledge and remaining questions. Oral oncol 2011; 47: 1099-104.

[45] Chiapasco M, Abati S, Ramundo G, Rossi A, Romeo E, Vogel G. Behavior of implants in bone grafts or free flaps after tumor resection. Clin Oral Implants Res 2000; 11: 66-75.

[46] Vannabouathong C, Sprague S, Bhandari M. Guidelines for fracture healing assessments in clinical trials. Part I: Definitions and endpoint committees. Injury 2011; 42: 314-6.

[47] Ishida S, Shibuya Y, Kobayashi M, Komori T. Assessing stomatognathic performance after mandibulectomy according to the method of mandibular reconstruction. Int J Oral Maxillofac Surg 2015; 44: 948-55.

[48] Roumanas ED, Garrett N, Blackwell KE, Freymiller E, Abemayor E, Wong WK, Beumer J, 3rd, Fueki K, Fueki W, Kapur KK. Masticatory and swallowing threshold performances with conventional and implant-supported prostheses after mandibular fibula free-flap reconstruction. J Prosthet Dent 2006; 96: 289-97.

# Biomechanical Analysis of Bone Remodeling Following Mandibular Reconstruction using Fibula Free Flap

Nobuhiro Yoda*[1,2], Keke Zheng[2], Junning Chen[3], Zhipeng Liao[2], Shigeto Koyama[4], Christopher Peck[5], Michael Swain[6], Keiichi Sasaki[1], and Qing Li[2].

[1]Division of Advanced Prosthetic Dentistry, Tohoku University Graduate School of Dentistry, 4-1, Seiryo-machi, Aoba-ku, Sendai, Miyagi, 9808575, Japan

[2]School of Aerospace, Mechanical and Mechatronic Engineering, The University of Sydney, NSW 2006, Australia

[3]Department of Biomaterials, Max Planck Institute of Colloids and Interfaces, Am Mühlenberg 1 OT Golm, 14476 Potsdam, Germany

[4]Maxillofacial Prosthetics Clinic, Tohoku University Hospital, 1-1, Seiryo-machi, Aoba-ku, Sendai, Miyagi, 9808575, Japan

[5]Faculty of Dentistry, The University of Sydney, Sydney, NSW, 2006, Australia

[6]Department of Bioclinical Sciences, Faculty of Dentistry, Kuwait University, Safat 13110, Kuwait

*** Corresponding Author: Nobuhiro Yoda**

**Contact details:**

Address: Division of Advanced Prosthetic Dentistry, Tohoku University Graduate School of Dentistry, 4-1, Seiryo-machi, Aoba-ku, Sendai, Miyagi, 9808575, JAPAN

Phone: +81-22-717-8369; Fax: +81-22-717-8371;

E-mail: nobuhiro.yoda.e2@tohoku.ac.jp

# Abstract

Whilst the newly established biomechanical conditions following mandibular reconstruction using fibula free flap can be a critical determinant for achieving favorable bone union, little has been known about their association in a time-dependent fashion. This study evaluated the bone healing/remodeling activity in reconstructed mandible and its influence on jaw biomechanics using CT data, and further quantified ~~its~~ their correlation with mechanobiological responses through an *in-silico* approach. A 66-year-old male patient received mandibular reconstruction was studied. Post-operative CT scans were taken at 0, 4, 16 and 28 months. Longitudinal change of bone morphologies and mineral densities were measured at three bone union interfaces (two between the fibula and mandibular bones and one between the osteotomized fibulas) to investigate bone healing/remodeling events. Three-dimensional finite element models were created to quantify mechanobiological responses in the bone at these different time points. Bone mineral density increased rapidly along the bone interfaces over the first four months. Cortical bridging formed at the osteotomized interface earlier than the other two interfaces with larger shape discrepancy between fibula and mandibular bones. Bone morphology significantly affected mechanobiological responses in the osteotomized region ($R^2$>0.77). The anatomic position and shape discrepancy at bone union affected the bone healing/remodeling process.

**Keywords:** Fibula free flap; Finite element analysis; Jaw biomechanics; Mandibular reconstruction; Bone remodeling.

## 1. Introduction

Free vascularized osteocutaneous tissue transfer has become a well-established procedure for maxillomandibular reconstruction following large resection due to trauma, atrophy, and tumors ablation [1,2]. Fibula free flap (FFF) provides superior length and long vascular pedicles for mandibular reconstruction, with proven subsequent high reliability and adaptability [3]. Nevertheless, some clinical complications remain with delayed or poor union between the grafted fibula bone and host native mandible [4,5]. Recent CT evaluations reported 20% [6] and 9% [7] non-union rates, respectively. Bone union determines the strength and health of the reconstructed mandible, both of which are essential for further ~~kono~~occlusal and prosthetic rehabilitation. In the case of bone fracture healing, the mechanobiological environment, which is thought to regulate cellular behaviors, can be a critical determinant [8].

Unlike general bone fracture healing processes, FFF mandibular reconstruction may be affected by additional factors, such as shape discrepancy between different bones and poor bone vascularity [4,9]. Further, the loss of several masticatory muscles due to resection can cause unbalanced jaw movement and abnormal mastication, leading to significant change in the biomechanical conditions [10,11]. Thus the mechanobiological responses in the jaw can be altered significantly; and such a change in-turn affects subsequent bone remodeling activities [12,13]. To assist surgical planning and oral rehabilitation it is essential to understand bone healing/remodeling activity and its influence on jaw biomechanics, thereby preventing delayed or poor union of bone grafts.

Finite element (FE) analysis has the adequacy for the biomechanical studies on orthopaedic [14-16] and dental problems [17-19]. Several those studies demonstrated their compelling advantages for understanding the biomechanics and mechanobiology of reconstructed mandibles *in-silico* [20,21]. ~~Several finite element (FE) studies demonstrated their compelling advantages for understanding the biomechanics and mechanobiology of reconstructed mandibles [14,15].~~ With recent advances in micro computerized tomography (CT), bone mineral density (BMD) and morphological changes can be measured to evaluate bone remodeling sequences noninvasively [~~16,17~~13,22,23]. The CT-based 3D FE models can be thus created to quantify biomechanical responses to functional forces in a patient-specific and time-dependent manner [~~13,18~~24,25].

This study aims to (1) examine longitudinal changes in bone morphology and mineral density in the course of healing/remodeling after mandibular reconstruction with FFF; and (2) investigate the associated variation in mandibular biomechanics in terms of mechanical stimulus. The postoperative CT scans were performed at 4 critical time points over two and half years' clinical follow-up, and the CT images were segmented for both 2D multiple planar reconstructions (MPR) and 3D (volumetric) analyses. The bone condition was analyzed in both spatial and temporal manner, in terms of morphology and BMD. Nonlinear 3D FE analyses were conducted to quantify the bone mechanobiological stimuli at these different time points; and then correlated to the corresponding *in-vivo* clinical data. By establishing this combined *in-vivo* and *in-silico* approach, the mutual influence between tissue conditions and mandibular mechanobiology was assessed. The results are expected to provide important insights into surgical plan for mandibular reconstruction.

# 2. Materials and Methods

### *2.1 Clinical Treatment*

A 66-year-old male patient received mandibular reconstruction with osteotomized FFF, due to a squamous-cell carcinoma at the right molar gingiva at the Department of Otolaryngology-Head and Neck Surgery, Tohoku University Hospital in Japan. Upon harvesting, the fibular bone was segmented to match the defect jaw morphology. A titanium fixation plate (Synthes, Solothurn, Switzerland), which was pre-bent using the CT-based 3D patient model before surgery, was configured to be fixed monocortically with a total of 11 titanium screws (Synthes, Solothurn, Switzerland) as shown in Fig. 1. The first CT scan (M0) was performed at the end of surgery, and the follow-up CTs were taken at 4, 16 and 28 months after surgery (namely, M4, M16, and M28, respectively). A removable partial denture was inserted into this subject 6 months after the surgery; however, the subject did not use it for mastication, due to fear of biting on the reconstructed side. The periodontal conditions of the remaining teeth and the removable partial denture have been maintained at the Maxillofacial Prosthetics Clinic in Tohoku University Hospital every three months.

### *2.2 CT Imaging Acquisition and 2D Image Analysis*

Multi-detector helical CT scans were performed for the follow-up examinations using Somatom Emotion 6 (Siemens, Erlangen, Germany) at 120 kV and 80 mA with the spatial resolution of 0.4, 0.4, and 0.8 mm in the radial, tangential, and axial directions. The CT data was further processed with the medical image viewer software (EV Insite S, PSP Co., Tokyo, Japan), for the detection and alignment of anatomic landmarks between the different cross-sectional examinations. The mandibular plane was defined using three reference points; namely, left Gonion point, Menton point, and inflection point of a titanium fixation plate (green triangles in Fig. 2a). Six planes parallel to this mandibular plane were selected for the quantitative analysis of bone union at three docking sites (DS1, DS2, and DS3, respectively) with 2 mm intervals by multiple planar reconstructions (MPR) (Fig. 2b) [12]. On each plane, a 2 $mm^3$ volume of interest (VOI) was ~~placed~~ considered along the superior-inferior axis (Fig. 2b). Since a significant correlation between Hounsfield units (HU) obtained from clinical CT scans and bone mineral density (BMD) were ~~found~~ established [~~19~~26], the HU values change in VOIs can be regarded as the BMD changes over time here, particularly for bone unification at the contact interfaces. All the VOIs were placed at the same positions throughout these four time points, based on the distance from the titanium fixation plate and screws as a reference.

### *2.3 3D Registration and Volumetric Analysis*

3D registration was carried out for investigating the longitudinal changes in bone surface profile and mineral density using Amira 2016.22 (Zuse Institute Berlin (ZIB), Berlin, Germany) (Fig. 3a). The titanium fixation plate was selected as the reference geometry for its rigidness and high contrast. To quantify the variation of BMD at the docking sites, the change in greyscales was correlated with the distance from the inferior to the superior aspect. The average value of the pixel intensity (i.e. greyscale) was calculated in the cortical bone region on each slice (at a regular spacing of 0.8 mm along the coronal axis~~al~~), enabling a plot of pixel value change along the axial direction. To determine the HU values of the cortical bone, several profile lines were constructed at the CT images cross the region of mature cortical bone. By sampling the histogram distribution, a HU value of 1536 was determined to be a threshold for determining cortical bone pixels, which is ~~in~~ consistent with the reported HU value of cortical bone for cone beam CT in literature [~~20~~27]. By using this cortical bone threshold, variation in both bone density and volume at the same region for the four time points were quantified. The detailed variation in bone volume (i.e. volume of the cortical bone voxel cuboids) along this direction was plotted using the same approach. In addition, the variation in pixel number, rather than the pixel intensity, in the cortical bone region was considered.

### *2.4 Finite Element Analysis*

Four case-specific FE models were created based on the CT data taken at M0, M4, M16, and M28, respectively [~~21,22~~28,29]. The CT images were imported into ScanIP Ver. 4.3 (Simpleware Ltd, Exeter, UK) for segmentation. The segmented masks (bone, individual tooth and titanium fixation plate) were further processed in Rhinoceros 4.0 (Robert McNeel & Associates, Seattle, USA) to create parametric models with non-uniform rational B-spline (NURBS) (Fig. 3b). Following the development of the mandibular models, the total 11 fixation screws were modeled according to the manufacturing specifications in Solidworks 2013 (SolidWorks Corp, Waltham, MA, USA). Those screws were virtually inserted into the models in Rhinoceros 4.0 as guided by the CT images. Considering that the patient disuse the denture in his daily life and has no parafunctional habit, the denture was not inserted in the models. To ensure the numerical accuracy, an adaptive mesh was generated based on a mesh convergence test. Ten-node ~~Q~~quadratic tetrahedral elements with hybrid formulation (C3D10H) were adopted to ensure smoothness along the contact interfaces.

A pixel-based mapping algorithm was adopted to create the heterogeneous bone density distributions at the different time points, reflecting the changes of the anatomical conditions [29].[22] A homogeneous isotropic linear-elastic model was used to define the teeth (Young's modulus E =20,000 MPa, Poisson's ratio ν =0.2), titanium fixation plates and screws (Ti6Al7Nb: E=110,000 MPa, ν=0.3) [15,2321,30].

The hinge constraints were prescribed for the corresponding mandibular condyles. In this subject, the large bone resection was accompanied by the functional loss of the right masseter, medial pterygoid and temporalis muscles; and consequently masticatory conditions changed dramatically post-surgery. Due to lack of information regarding muscular forces after such a large resection [1420], the magnitudes and directions of individual forces were derived based on the literature for the remaining muscles (masseter mascle: 59.23 N, medial pterygoid muscle: 39.60 N, lateral pterygoid muscle: 34.44 N, and temporalis: 34.09 N, respectively) [2431].

Strain energy density (SED) was quantified as a mechanobiological stimulus to analyze the bone responses in the three docking sites and VOIs. SED has been considered an effective stimulus to bone remodeling in long bones [32] and mandible [24,33] and can be a scalar quantity to combine stress and strain but eliminate their directionalities [34]. The SEDs at different time points were correlated with the corresponding change in the bone density. In this study, linear regression analysis was performed using IBM SPSS Statistics Ver. 21.0 (IBM Corp., New York, NY, USA) to examine the correlations between stimuli and bone remodeling progression in all VOIs. The $R^2$ values presented the goodness of fit for the predictor functions, thereby indicating the extent of correlation.

# 3. Results

### *3.1 MPR Image Assessment for Bone Morphology and Mineral Density*

Fig. 4 shows the longitudinal changes in bone profile from the CT-based MPR images. In docking site DS1, a significant amount of callus bone formed at time point M4, and the cortical bridging successfully formed in both buccal and lingual regions at M16. In DS2, the cortical bridging formed at M4 in both the buccal and lingual regions. Also, the cortical-like bone appeared to fill the entire interface, while some resorption occurred at the upper and bottom surfaces of cortical bone. In DS3, there was large discrepancy of bone shape at the initial stage. However, the bone shapes gradually remodeled and cortical bridging was found in both the buccal and lingual regions at M16.

Fig. 5 shows that the averaged HU value was calculated for each VOI to quantify the change of BMD.~~Averaged HU value was calculated for each VOI to quantify the change of BMD (charts in Fig. 4).~~ For DS1, both superior and inferior cortical bones underwent resorption from M0 to M16, while the BMD peaked in the trabecular interface regions at M4 before undergoing resorption. In contrast, the grafted bones at DS2 performed exceedingly well in terms of new bone formation, despite being osteotomized, ~~with~~ seen in rapid increases of BMD in the first four months. For DS3, the cancellous/trabecular region underwent much more ~~severe~~ dramatic remodeling than the cortical bone with rapid increase in BMD from M0 to M4 but decrease from M4 to M16.

### *3.2 Volumetric Assessment of Bone Mineral Density and Morphology*

Bone morphological changes were visualized as the apposition and resorption on the bone surface by 3D volumetric registration in the three docking sites (Fig. ~~5a-c~~6). The longitudinal changes in bone volume were site-specific and the rate of volume increase in the cortical bone region was positive in all the three sites from M4 to M16 (Fig. ~~5d~~7a). Fig. ~~5e~~ 7b exhibits the longitudinal change rate of bone volume at each docking site. Bone volume increased remarkably from M4 to M16 due to new bone formation, especially at the region from 15 mm to 25 mm for DS1 and from 20 mm to 30 mm for DS3 on the sectional plane of mandible as visualized in Fig. ~~5a-c~~6. Fig. ~~5f~~ 7c plotted the site-specific change rate of BMD based on the average grayscale in the cortical bone region. Note that the BMD decreased in the first four months for all the docking sites.

### *3.3 Mechanobiological Stimulus Distribution*

Fig. ~~6a~~ 8 shows the longitudinal changes in the SED distribution and corresponding CT MPR images of the reconstructed mandible. Both global and local SED distributions changed ~~significantly~~ with time significantly. The longitudinal changes in morphology and BMD were remarkable particularly for DS1, leading to substantial variation in the SED distribution.

The SED at VOIs in the cortical bone region was generally higher than that in the cancellous region in DS1 and DS2 (Fig. ~~6b~~9). At each VOI, the SED decreased with time at DS1 and DS3, especially in the superior region of DS1. While the increase in SED with time could be found in some VOIs, the SED dropped from M0 to M4 and then gradually increased till M28 (but never exceeds that at M0), at 6, 8, and 10 mm

VOIs in DS2.

Linear regression analysis between the HU values and SED in VOIs indicated that there was a strong dependence on the HU values only in DS2 ($p<0.05$), as shown in Fig. 10.

## 4. Discussion

Both 2D MPR images and 3D volumetric analyses enabled to quantify and visualize time-dependent bone apposition and resorption in terms of morphology and BMD in this FFF reconstructive mandible. This study is believed to be the first of its kind for investigating the anatomical sequence of healing/remodeling process and its correlation with mechanobiological responses in a reconstructive mandible.

The clinical process of cortical bridging at bone docking regions was found to be significantly site-specific based on the results of both 2D MPR images and 3D volumetric analyses. Biological healing at bone union is influenced by complex cellular and molecular activities, and can be affected by the dimension of bone segment gap [~~25~~35] and contact shape [9]. In this study, we set up a criterion to justify the cortical bridging, namely, no gap was observed between the two bones in the six cross sectional planes as shown in Fig. 4. According to this criterion, the contact region in DS2 achieved earlier cortical bridging than the other two sites.~~Specifically, the contact region in DS2 achieved earlier cortical bridging than the other two sites (Fig. 4).~~

The BMD became higher within the first four months in all the VOIs except for the cortical bone regions in DS1 (Fig. ~~4~~5). Those cortical regions appeared to undergo significant resorption, while the osseous callus was generally found at the interface of trabecular regions during the bone-healing phase [~~26,27~~36,37]. The BMDs of all the cortical bone regions in the docking sites were also found to decrease in the first four months, which was most remarkable for DS2 (Fig. ~~5f~~7c). Despite a vascularized bone graft, the lower bone vascularity may have caused the reduction of BMD on the cortical region of the fibula graft [~~28,29~~38,39]. Despite the lowered BMD, 3D volumetric analysis revealed a higher increase rate of bone volume in DS1 than the other two sites over the same time period (Fig. ~~5d~~7a). Primary bone apposition may have developed throughout formation of the osseous callus at the endochondral and periosteal areas (Figs. ~~4a~~4 and 5) [~~25~~35]. The woven bone with low BMD appears to initially form for filling the gap and reducing morphological discrepancy, which may be related to the initial volume increase in DS1. Lamellae bone with high BMD appears to form after M4 [~~27~~37]. Lower bone vascularity in the distal segment of osteotomy [~~29~~39] may limit those biological healing activities in DS2 and DS3 compared to DS1, further contributing to the initial reduction in the bone volume (Fig. ~~5d~~7a).

Considering the positive increase rates attributable to bone apposition at all three docking sites from M4 to M16, bone (re)modeling activity had a primary effect on post-healing bone formation [~~30,31~~40,41]. Osseous callus at the interface regions in DS1 and DS3 gradually became cancellous bone, forming a natural mandibular structure during the course. Nevertheless, the healing and remodeling process at the docking site, especially with large shape discrepancy, is considered to be significantly slower than those of the general bone fracture [~~27,32~~37,42]. Note that the mandible can be distorted during daily oral function [~~33~~43]. Despite the mechanical fixation by titanium plate, the distortion can affect the mechanical stability of the docking sites, which might also delay the healing process [9].

Mechanical loading is known to stimulate bone healing and remodeling process, likely enhancing bone mass and functionality [~~30~~40]. The mechanobiological impetus can thus be related to the bone remodeling activity [12,13]. SED has been considered an effective stimulus to bone remodeling in long bones [~~34~~32] ~~and~~ as well as mandible [~~18,35~~24,33]. This study revealed the correlation between SED and healing/remodeling outcome over the time period concerned.

The variation in SED distribution was attributed to the time longitudinal change in the mandibular morphology (Figs. ~~6~~8 and 9), as well as load transfer in the restructured mandible, particularly through the fibula grafts. In other words, the functional load was initially transferred to the fibula graft completely via the titanium fixation plate (M0); but subsequently, a greater proportion of load transferred through the bony tissue as the extent of bone union increased. In addition, the remaining unbalanced muscle activities readapt with time [10,11]. All these factors have a collective effect on the mechanobiological responses.

As shown in Fig. ~~7~~10, the SED had a strong dependence on the HU values in DS2 ($p<0.05$). The HU value altered the load bearing capability of the fibula bone, meaning that the SED is associated with HU values. Lower bone vascularity and good bone contact condition at DS2 possibly enhance the effect of mechanobiological stimuli on BMD adaptation, which might be related to the earlier process of cortical bridging at the DS2. For DS1 and DS3, significant shape discrepancy due to reconstruction generated non-physiological stress/strain concentration, which might have distorted the distribution of SED and its correlation to remodeling.

Clinically, the implant-supported denture is considered as the most suitable option for functional rehabilitation following mandibular reconstruction [2]. Although the timing of implant placement is still controversial, several studies adopted the time for implant placement at least 6–-12 months after the reconstruction with FFF [1,36,3744,45]. Considering the cortical bridging as a predictor of bone union strength [7,3846], all the bone unions can be confirmed through CT scanning, especially in the cases with a large bone discrepancy. Specifically, favorable initial bone contacts with small shape discrepancy are considered a primary factor for earlier success of cortical bridging.

There are still some limitations in this study. Constrained by the clinical protocol and radiation dosage allowance, the scanning resolution of CTs could have affected modeling accuracy. The FE analyses still included several assumptions, such as simulation under static loading conditions and rotational movement on the mandibular condyles. The applied muscle forces did not precisely reflect specific condition of this subject; plus the muscle forces are anticipated to change over time after reconstruction [39,4047,48]. Consequently, the resultant reaction responses on both temporomandibular joints might become asymmetric and physiologically complicated. Finally, while the study was featured as patient-specific, the results were based on only one particular subject. In addition, other patient's factors, such as the systematic background and the treatment process, could be generally the decisive factors to the bone healing and remodeling process at the docking sites. Further evaluation and data acquisition of other subjects with inevitably varied conditions are necessary before generalizing these clinical and biomechanical findings.

## 5. Conclusion

This newly developed ~~analysing methods~~analysis procedure provided a quantitative clinical follow-up of mandibular reconstruction with fibula free flap (FFF) and fundamental understanding of time-dependent biomechanical responses in the reconstructed mandible. It was found that the bone healing and remodeling process at the docking sites were site-specific; and cortical bridging in the osteotomized region took place faster than that in the other docking sites between mandibular and fibula bones for the specific patient concerned. Within the limitation of this study, the anatomic position and the discrepancy of initial shape at the docking sites between the host mandible and fibula graft affected the bone healing and remodeling process. It ~~revealed~~ divulged a correlation between mechanobiological stimulus (strain energy density - SED) and the longitudinal change in bone mineral density (BMD) and morphology, especially at the osteotomized region. The longitudinal CT data and mechanobiological correlation generated in this study provided new insights into patient-specific surgical planning and occlusal rehabilitation.

## Conflict of interests

None declared.

## Ethical approval

The research protocol was approved by the research ethics committee of the Tohoku University Graduate School of Dentistry (reference #24-10). Full written informed consent was obtained to use the CT images for this study. All procedures performed in this study were in accordance with the ethical standards of the 1964 Helsinki Declaration (http://www.wma.net) and its later amendments.


## Acknowledgements

This work was supported by the Australian Research Council (ARC) through the Discovery and Fellowship schemes (DP160104602 and FT120100947). We are grateful to Dr. Atsushi Takeda and Dr. Naoko Sato at Tohoku University Hospital for providing and caring for this study patient.

# References

[1] Hakim SG, Kimmerle H, Trenkle T, Sieg P, Jacobsen HC. Masticatory rehabilitation following upper and lower jaw reconstruction using vascularised free fibula flap and enossal implants-19 years of experience with a comprehensive concept. Clin Oral Invest 2015; 19: 525-34.

[2] Chiapasco M, Biglioli F, Autelitano L, Romeo E, Brusati R. Clinical outcome of dental implants placed in fibula-free flaps used for the reconstruction of maxillo-mandibular defects following ablation for tumors or osteoradionecrosis. Clin Oral Implants Res 2006; 17: 220-28.

[3] Hidalgo DA, Rekow AA. Review of 60 consecutive fibula free flap mandible reconstructions. Plast Reconstr Surg 1995; 96: 585-96.

[4] Virgin FW, Iseli TA, Iseli CE, Sunde J, Carroll WR, Magnuson JS, Rosenthal EL. Functional outcomes of fibula and osteocutaneous forearm free flap reconstruction for segmental mandibular defects. Laryngoscope 2010; 120: 663-7.

[5] Nam W, Kim HJ, Choi EC, Kim MK, Lee EW, Cha IH. Contributing factors to mandibulotomy complications: A retrospective study. Oral Surg Oral Med Oral Pathol Oral Radio Endod 2006; 101: e65-70.

[6] Yla-Kotola TM, Bartlett E, Goldstein DP, Armstrong K, Gilbert RW, Hofer SOP. Union and bone resorption of free fibular flaps in mandibular reconstruction. J Reconstr Microsurg 2013; 29: 427-32.

[7] Akashi M, Hashikawa K, Kakei Y, Sakakibara A, Hasegawa T, Minamikawa T, Komori T. Sequential evaluation for bone union of transferred fibula flaps in

reconstructed mandibles: Panoramic x-ray versus computed tomography. Int J Oral Maxillofac Surg 2015; 44: 942-7.

[8] Gerstenfeld LC, Cullinane DM, Barnes GL, Graves DT, Einhorn TA. Fracture healing as a post-natal developmental process: Molecular, spatial, and temporal aspects of its regulation. J Cell Biochem 2003; 88: 873-84.

[9] Feron JM, Mauprivez R. Fracture repair: General aspects and influence of osteoporosis and anti-osteoporosis treatment. Injury 2016; 47 Suppl: 10-4.

[10] Hannam AG, Stavness IK, Lloyd JE, Fels SS, Miller AJ, Curtis DA. A comparison of simulated jaw dynamics in models of segmental mandibular resection versus resection with alloplastic reconstruction. J Prosthet Dent 2010; 104: 191-8.

[11] Namaki S, Morimoto M, Ohba H, Tanaka H, Koshikawa N, Shinohara M. Masticatory efficiency before and after surgery in oral cancer patients: Comparative study of glossectomy, marginal mandibulectomy and segmental mandibulectomy. J Oral Sci 2004; 46: 113-7.

[12] Suenaga H, Chen J, Yamaguchi K, Li W, Sasaki K, Swain M, Li Q. Mechanobiological bone reaction quantified by positron emission tomography. J Dent Res 2015; 94: 738-44.

[13] Chen J, Ahmad R, Suenaga H, Li W, Swain M, Li Q. A comparative study on complete and implant retained denture treatments - a biomechanics perspective. J Biomech 2015; 48: 512-9.

[14] Mercuri EGF, Daniel AL, Hecke MB, Carvalho L. Influence of different

mechanical stimuli in a multi-scale mechanobiological isotropic model for bone remodelling. Med Eng Phys 2016; 38: 904-10.

[15] Yamako G, Chosa E, Zhao X, Totoribe K, Watanabe S, Sakamoto T, Nakane N. Load-transfer analysis after insertion of cementless anatomical femoral stem using pre- and post-operative CT images based patient-specific finite element analysis. Med Eng Phys 2016; 36: 694-700.

[16] Zheng K, Scholes C, Chen J, Parker D, Li Q. Multiobjective optimization of cartilage stress for non-invasive, patient-specific recommendations of high tibial osteotomy correction angle. Med Eng Phys 2017; 42: 26-34.

[17] Odin G, Savoldelli C, Bouchard PO, Tillier Y. Determination of Young's modulus of mandibular bone using inverse analysis. Med Eng Phys 2010; 32: 630-37.

[18] Bonnet AS, Postaire M, Lipinski P. Biomechanical study of mandible bone supporting a four-implant retained bridge Finite element analysis of the influence of bone anisotropy and foodstuff position. Med Eng Phys 2009; 31: 806-15.

[19] Haiat G, Wang HL, Brunski J. Effects of biomechanical properties of the bone-implant interface on dental implant stability: from in silico approaches to the patient's mouth. Annu Rev Biomed Eng 2014; 16: 187-213.

~~[13]~~

~~[14]~~ [20] Narra N, Valasek J, Hannula M, Marcian P, Sandor GK, Hyttinen J, Wolff J. Finite element analysis of customized reconstruction plates for mandibular continuity defect therapy. J Biomech 2014; 47: 264-8.

~~[15]~~ [21] Tie Y, Wang DM, Ji T, Wang CT, Zhang CP. Three-dimensional finite-element analysis investigating the biomechanical effects of human mandibular reconstruction with autogenous bone grafts. J Craniomaxillofac Surg 2006; 34: 290-8.

~~[16]~~ [22] Birkhold AI, Razi H, Weinkamer R, Duda GN, Checa S, Willie BM: Monitoring in vivo (re)modeling: A computational approach using 4d microct data to quantify bone surface movements. Bone 2015; 75: 210-21.

~~[17]~~ [23] Lukas C, Ruffoni D, Lambers FM, Schulte FA, Kuhn G, Kollmannsberger P, Weinkamer R, Muller R. Mineralization kinetics in murine trabecular bone quantified by time-lapsed in vivo micro-computed tomography. Bone 2013; 56: 55-60.

[24] Rungsiyakull C, Chen J, Rungsiyakull P, Li W, Swain M, Li Q. Bone's responses to different designs of implant-supported fixed partial dentures. Biomech Model Mechanobiol 2015; 14: 403-11.

[25] C Field, Q Li, W Li, M Thompson, M Swain. Prediction of mandibular bone remodelling induced by fixed partial dentures. J Biomech 2010; 43: 1771-9.

~~[18]~~

~~[19]~~ [26] Schreiber JJ, Anderson PA, Rosas HG, Buchholz AL, Au AG. Hounsfield units for assessing bone mineral density and strength: A tool for osteoporosis management. J Bone Joint Surg 2011; 93a: 1057-63.

~~[20]~~ [27] Reeves TE, Mah P, McDavid WD. Deriving hounsfield units using grey levels in cone beam CT: a clinical application. Dentomaxillofac Radiol 2012; 41:

500-8.

~~[21]~~ [28] Yoda N, Liao Z, Chen J, Sasaki K, Swain M, Li Q. Role of implant configurations supporting three-unit fixedpartial denture on mandibular bone response: biological-data-based finite element study. J Oral Rehabil 2016; 43: 692-701.

~~[22]~~ [29] Liao Z, Chen J, Zhang Z, Li W, Swain M, Li Q. Computational modeling of dynamic behaviors of human teeth. J Biomech 2015; 48: 4214-20.

~~[23]~~ [30] Chen J, Li W, Swain MV, Ali Darendeliler M, Li Q. A periodontal ligament driven remodeling algorithm for orthodontic tooth movement. J Biomech 2014; 47: 1689-95.

[31] Cruz M, Wassall T, Toledo EM, Barra LP, Lemonge AC. Three-dimensional finite element stress analysis of a cuneiform-geometry implant. Int J Oral Maxillofac Implants 2003; 18: 675-84.

[32] Huiskes R, Ruimerman R, van Lenthe GH, Janssen JD. Effects of mechanical forces on maintenance and adaptation of form in trabecular bone. Nature 2000; 405: 704-6.

[33] Lin D, Li Q, Li W, Duckmanton N, Swain M. Mandibular bone remodeling induced by dental implant. J Biomech 2010; 43: 287-93.

[34] Lin D, Li Q, Li W, Zhou S, Swain MV. Design optimization of functionally graded dental implant for bone remodeling. Composites Part B 2009; 40: 668-75.

~~[24]~~

~~[25]~~ [35] Ai-Aql ZS, Alagl AS, Graves DT, Gerstenfeld LC, Einhorn TA.

Molecular mechanisms controlling bone formation during fracture healing and distraction osteogenesis. J Dent Res 2008; 87: 107-18.

~~[26]~~ [36] Vanroermund PM, Romeny BMT, Schoonderwoert GJ, Brandt CJWM, Sijbrandij S, Renooij W. The use of computed-tomography to quantitate bone-formation after distraction epiphysiolysis in the rabbit. Skeletal Radiol 1987; 16: 52-6.

~~[27]~~ [37] Yuasa M, Mignemi NA, Barnett JV, Cates JM, Nyman JS, Okawa A, Yoshii T, Schwartz HS, Stutz CM, Schoenecker JG. The temporal and spatial development of vascularity in a healing displaced fracture. Bone 2014; 67: 208-21.

~~[28]~~ [38] Jacobsen C, Lubbers HT, Obwegeser J, Soltermann A, Gratz KW. Histological evaluation of microsurgical revascularized bone in the intraoral cavity: Does it remain alive? Microsurgery 2011; 31: 98-103.

~~[29]~~ [39] Chiodo AA, Gur E, Pang CY, Neligan PC, Boyd JB, Binhammer PM, Forrest CR. The vascularized pig fibula bone flap model: Effect of segmental osteotomies and internal fixation on blood flow. Plast Reconstr Surg 2000; 105: 1004-12.

~~[30]~~ [40] Birkhold AI, Razi H, Duda GN, Weinkamer R, Checa S, Willie BM. The influence of age on adaptive bone formation and bone resorption. Biomaterials 2014; 35: 9290-301.

~~[31]~~ [41] Christen P, Ito K, Ellouz R, Boutroy S, Sornay-Rendu E, Chapurlat RD, van Rietbergen B. Bone remodelling in humans is load-driven but not lazy. Nat Commun 2014; 5: 4855.

~~[32]~~ [42] Shirota T, Schmelzeisen R, Ohno K, Michi KI. Experimental reconstruction of mandibular defects with vascularized iliac bone grafts. J Oral Maxillofac Surg 1995; 53: 566-71.

~~[33]~~ [43] Korioth TWP, Hannam AG. Deformation of the mandible during simulated tooth clenching. J Dent Res 1994; 73: 56-66.

~~[34] Huiskes R, Ruimerman R, van Lenthe GH, Janssen JD. Effects of mechanical forces on maintenance and adaptation of form in trabecular bone. Nature 2000; 405: 704-6.~~

~~[35] Lin D, Li Q, Li W, Duckmanton N, Swain M. Mandibular bone remodeling induced by dental implant. J Biomech 2010; 43: 287-93.~~

~~[36]~~ [44] Anne-Gaelle B, Samuel S, Julie B, Renaud L, Pierre B. Dental implant placement after mandibular reconstruction by microvascular free fibula flap: Current knowledge and remaining questions. Oral oncol 2011; 47: 1099-104.

~~[37]~~ [45] Chiapasco M, Abati S, Ramundo G, Rossi A, Romeo E, Vogel G. Behavior of implants in bone grafts or free flaps after tumor resection. Clin Oral Implants Res 2000; 11: 66-75.

~~[38]~~ [46] Vannabouathong C, Sprague S, Bhandari M. Guidelines for fracture healing assessments in clinical trials. Part I: Definitions and endpoint committees. Injury 2011; 42: 314-6.

~~[39]~~ [47] Ishida S, Shibuya Y, Kobayashi M, Komori T. Assessing stomatognathic performance after mandibulectomy according to the method of mandibular reconstruction. Int J Oral Maxillofac Surg 2015; 44: 948-55.

[40] [48] Roumanas ED, Garrett N, Blackwell KE, Freymiller E, Abemayor E, Wong WK, Beumer J, 3rd, Fueki K, Fueki W, Kapur KK. Masticatory and swallowing threshold performances with conventional and implant-supported prostheses after mandibular fibula free-flap reconstruction. J Prosthet Dent 2006; 96: 289-97.

# Captions to illustrations

**Figure 1. Intraoperative view illustrating the fibula bone affixed to the titanium fixation plate.**

White triangle: mandibular bone, Black triangle: fibula bone. Green arrows: Screw position (8 of 11 screws are shown in this picture). The flap pedicles were anastomosed with the thyroid artery and the external jugular vein.

**Figure 2. Clinical X-ray and CT images for assessment.**

(a) Postoperative radiograph (M0). Yellow boxes: three investigated docking sites (DS1, DS2 and DS3) for the bone union. Green triangles: reference points for defining mandibular plane for 2D MPR (multiple planar reconstructions) analysis. (b) CT MPR cross-sectional images of contact interface perpendicular to the mandibular plane (green line in (b)) at three docking sites at M0; brown: mandible, yellow: anterior fragment of fibula bone, green: posterior fragment of fibula bone. Lateral lines: planes for analysis, boxes: cubic (2 $mm^3$) volume of interests (VOIs).

**Figure 3. Procedure of 3D image registration and computational model for finite element analysis.**

(a) Procedure of 3D image registration for investigating the longitudinal changes in bone surface profile and mineral density; the example for the DS1 between M0 model (orange) and M4 model (blue). Titanium fixation plate was selected as the reference geometry for the registration. (b) 3D modeling for the patient's jaw model (M0) with non-uniform rational B-spline (NURBS).

**Figure 4. MPR CT image analysis.**

(a) DS 1, (b) DS 2, (c) DS 3. Individual planes and VOIs are defined in Figure 2. Each plane position stated in terms of the distance from the bottom. Both top and bottom planes included the cortical bone region of fibula graft at M0.

**Figure 5. Time-dependent changes in HU value.**

(a) DS 1, (b) DS 2, (c) DS 3.

**Figure 6. Volumetric analysis of bone morphology changes by 3D image registration and superimposition**.

(a) DS 1, (b) DS 2, (c) DS 3

Figure 7. **Volumetric analysis of bone morphological changes.**

(a) Volume increase rate in the cortical bone region, (b) Site-specific volume change rate (%), (c) Site-specific BMD (greyscale) increase rate (%) based on the grayscale on the cortical bone region.

**Figure 8. Mechanobiological stimulus distributions.**

(a) M0, (b) M4, (c) M16, (d) M28. SED distribution was shown at the different time points and in different regions along with corresponding CT MPR images (anterior end of fibula graft in DS1 and posterior end of fibula graft in DS3).

**Figure 9. Average values of SED in each VOI assigned in the same location as in the CT MPR image.**

VOI position stated in terms of the distance from the bottom at each docking site shown in Fig. 2.

**Figure 10. Linear regression analysis between CT Hounsfield Unit (HU) and SED in volume of interests (VOIs)**

The VOIs were on the same location in each multiple planar reconstruction (MPR) image at each docking site shown in Fig. 2. *P < 0.05, **P < 0.01.

**Figure 1**


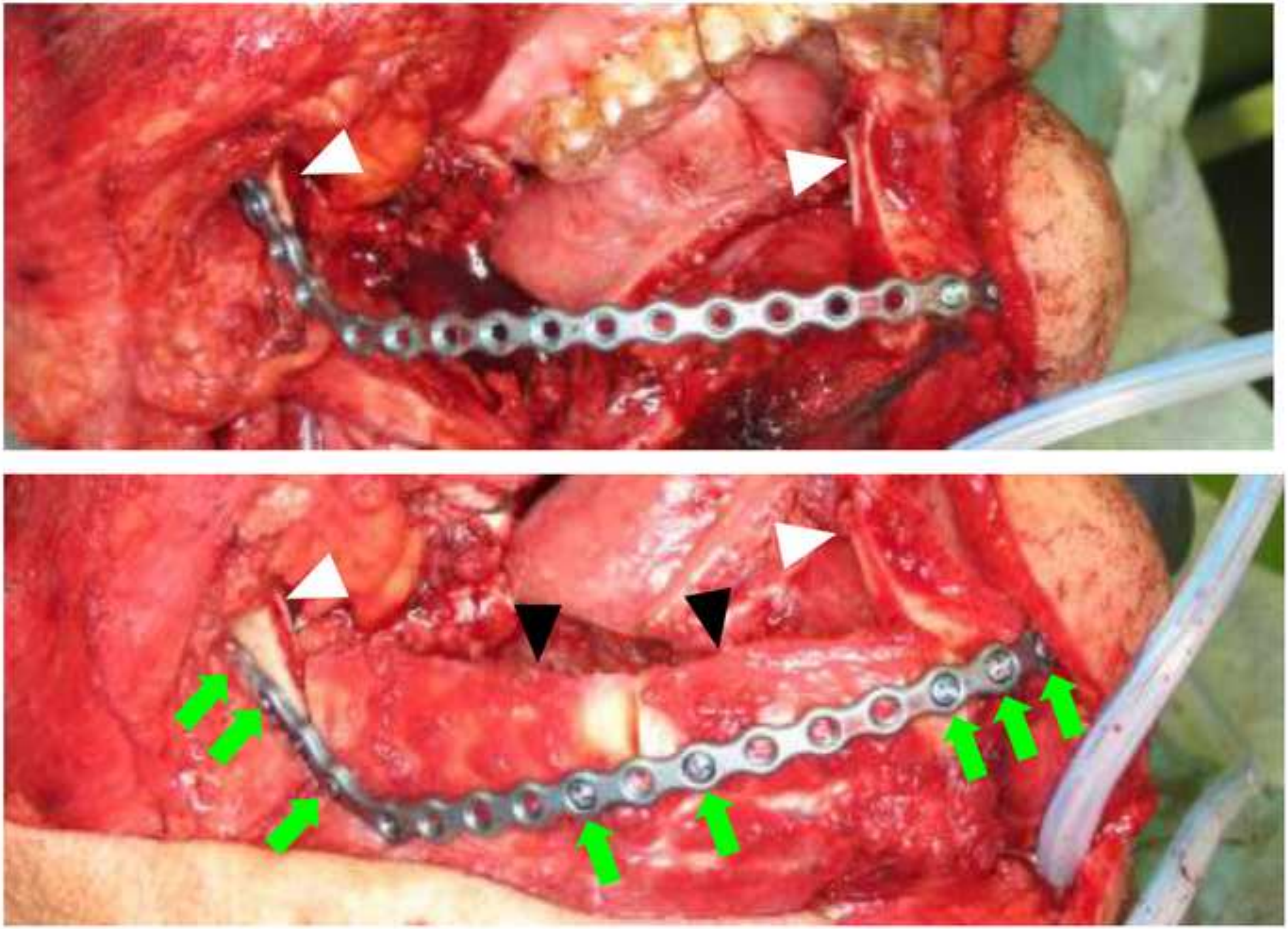

Figure 2
Click here to download high resolution image

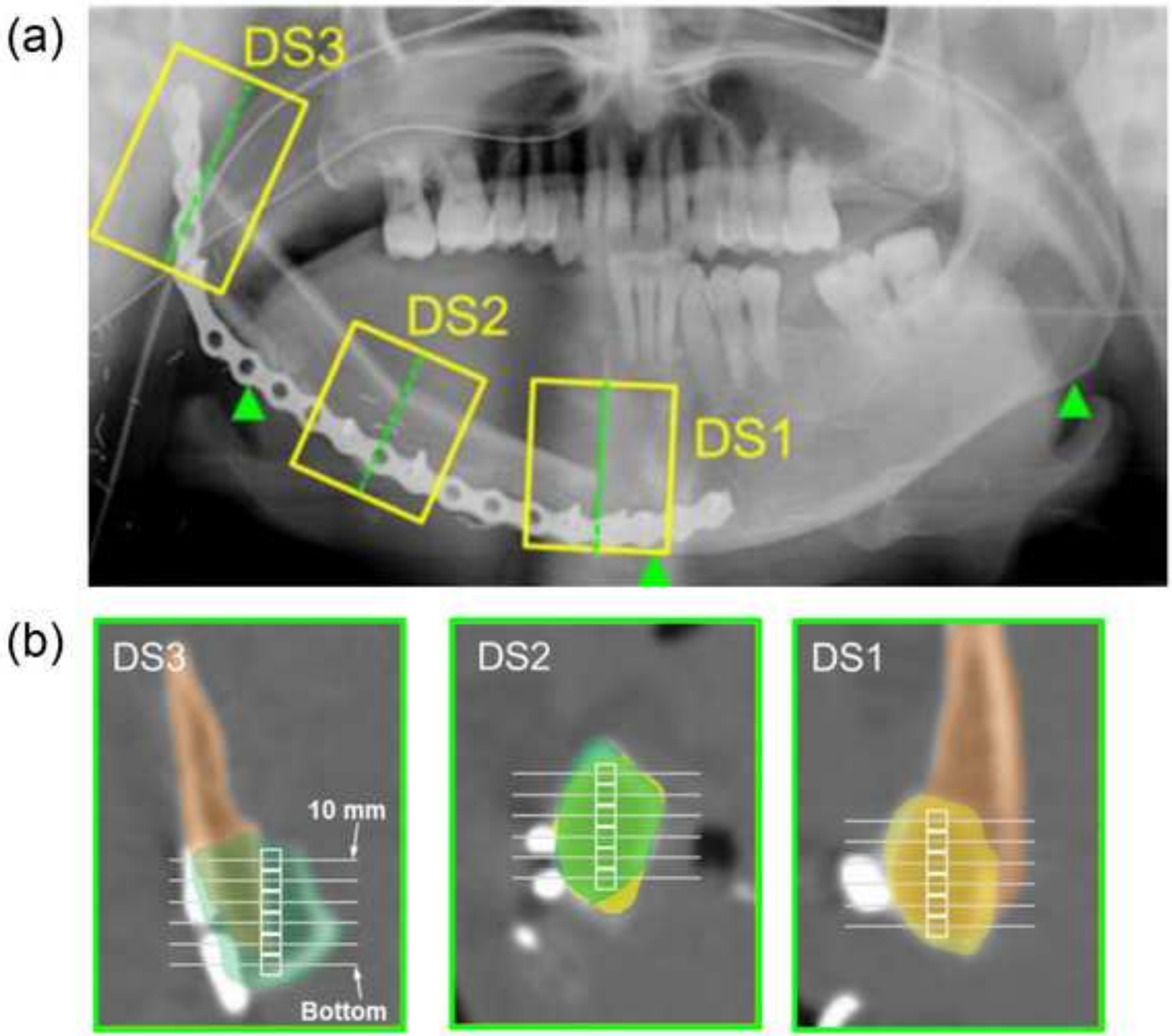

Figure 3
Click here to download high resolution image

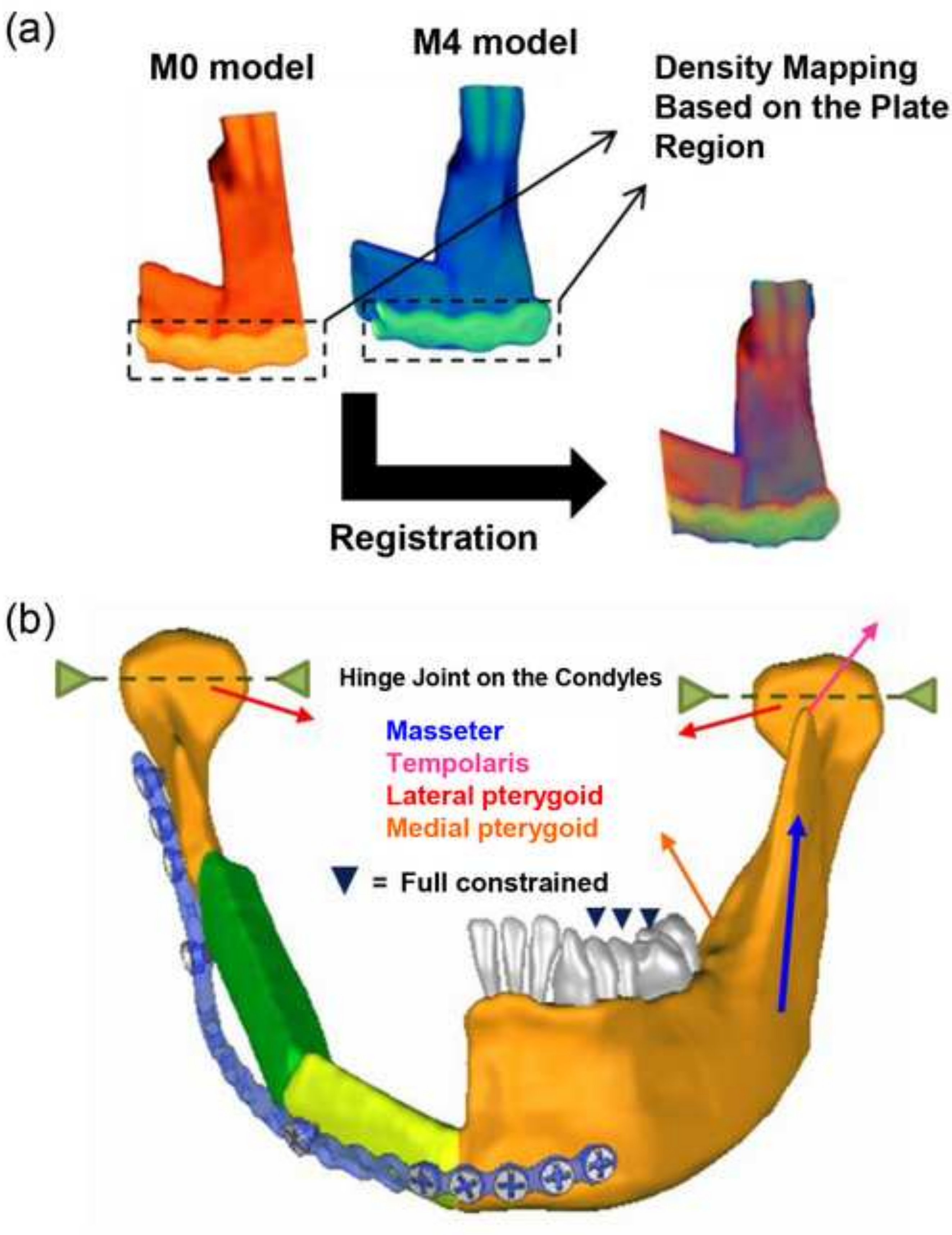

Figure 4
Click here to download high resolution image

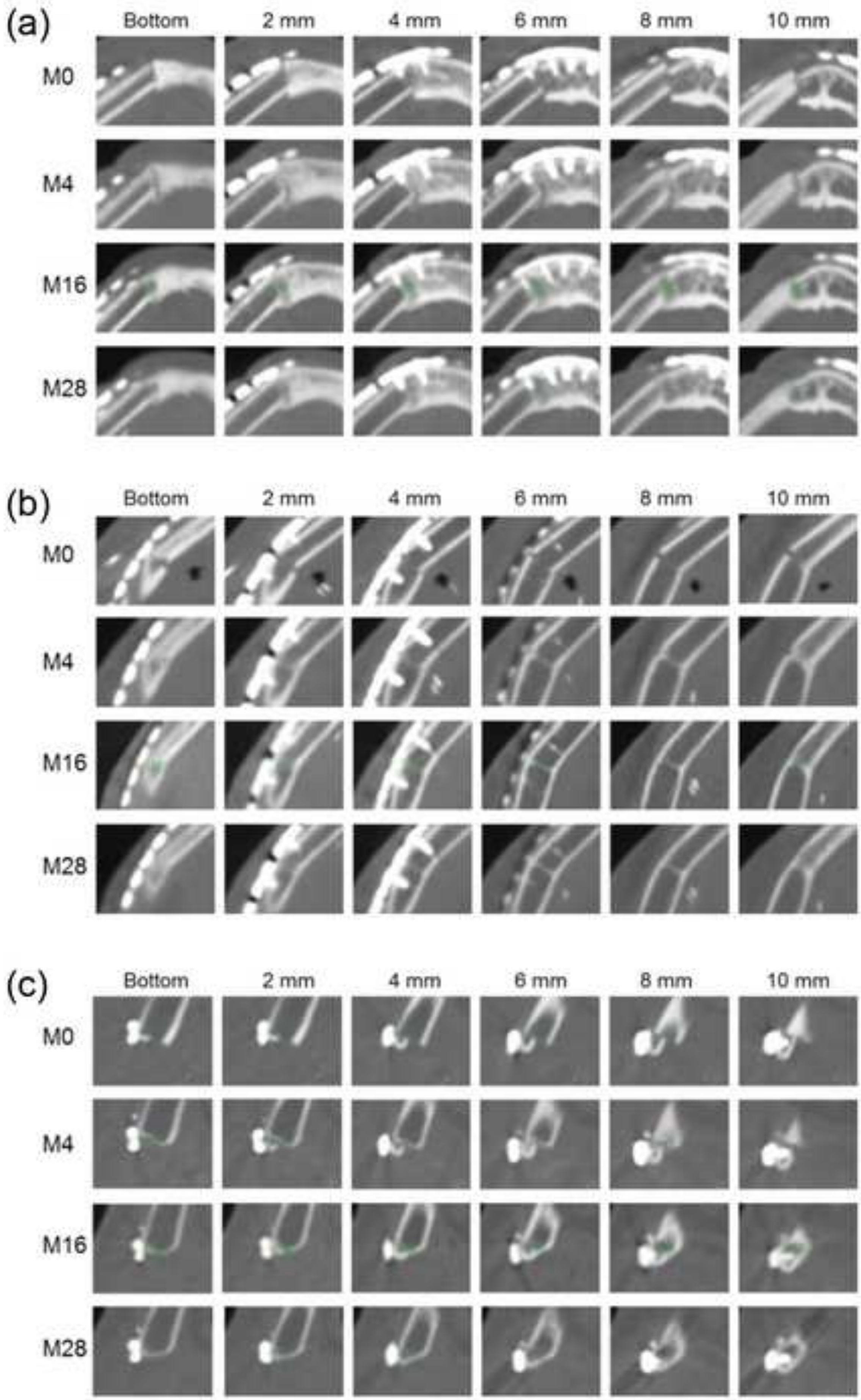

Figure 5
Click here to download high resolution image

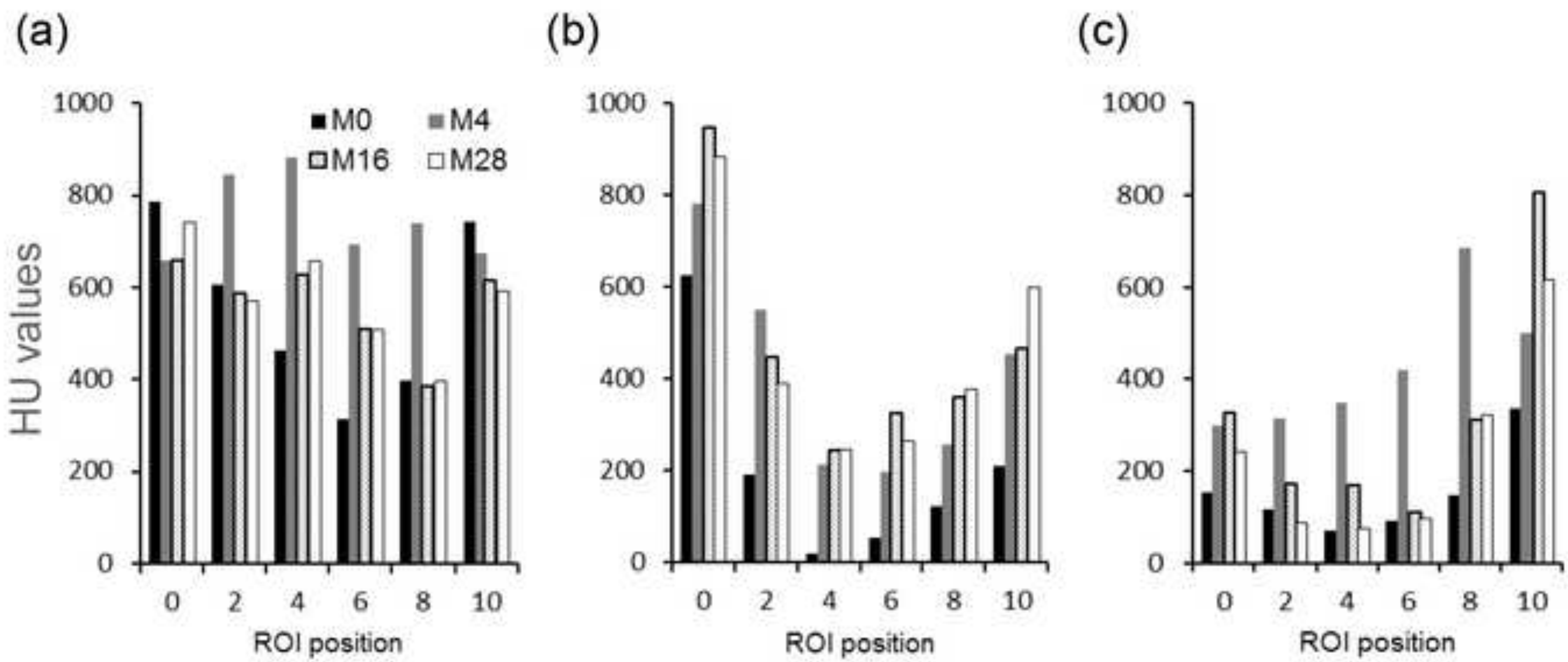

Figure 6
Click here to download high resolution image

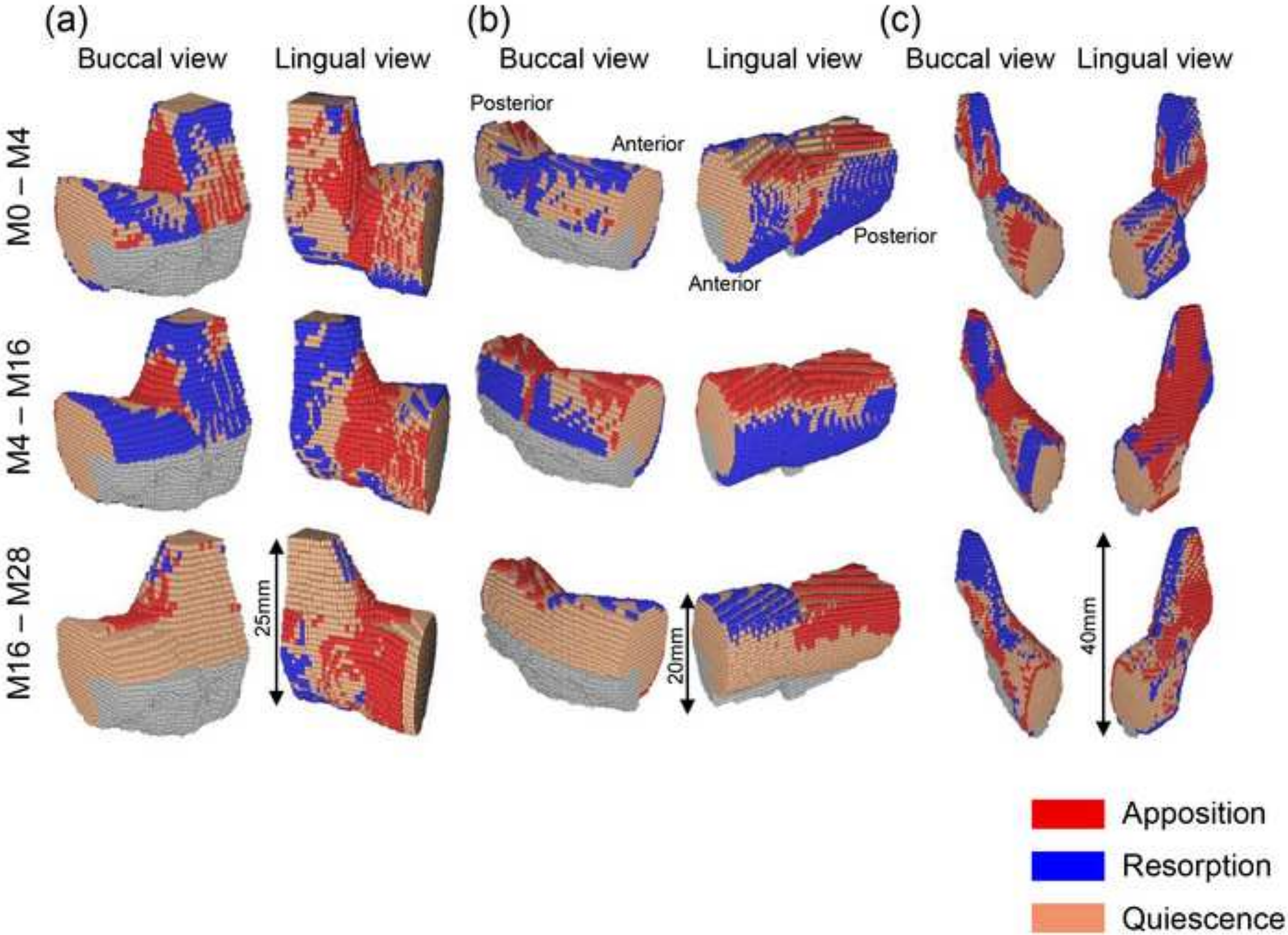

Figure 7
Click here to download high resolution image

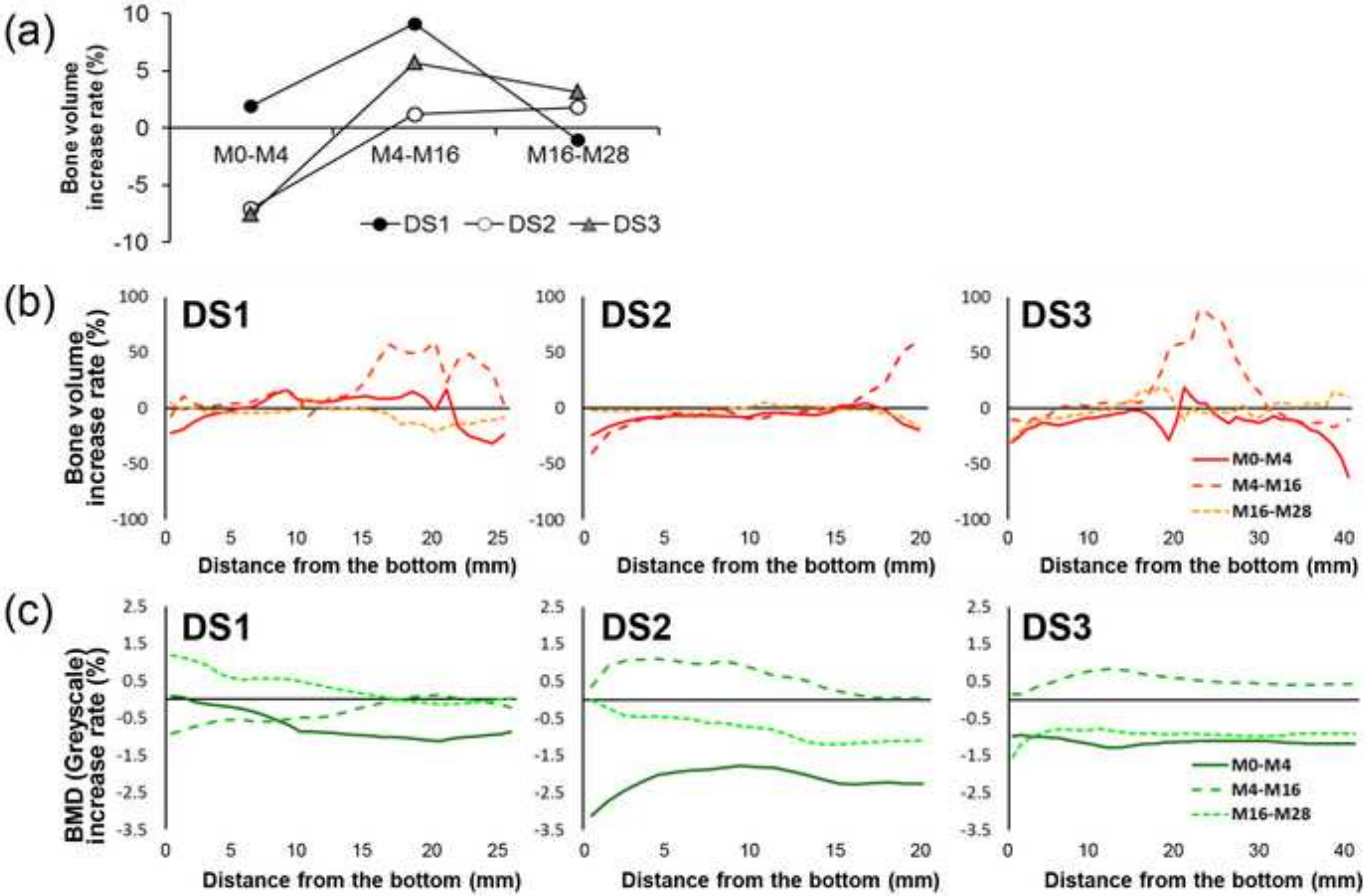

Figure 8
Click here to download high resolution image

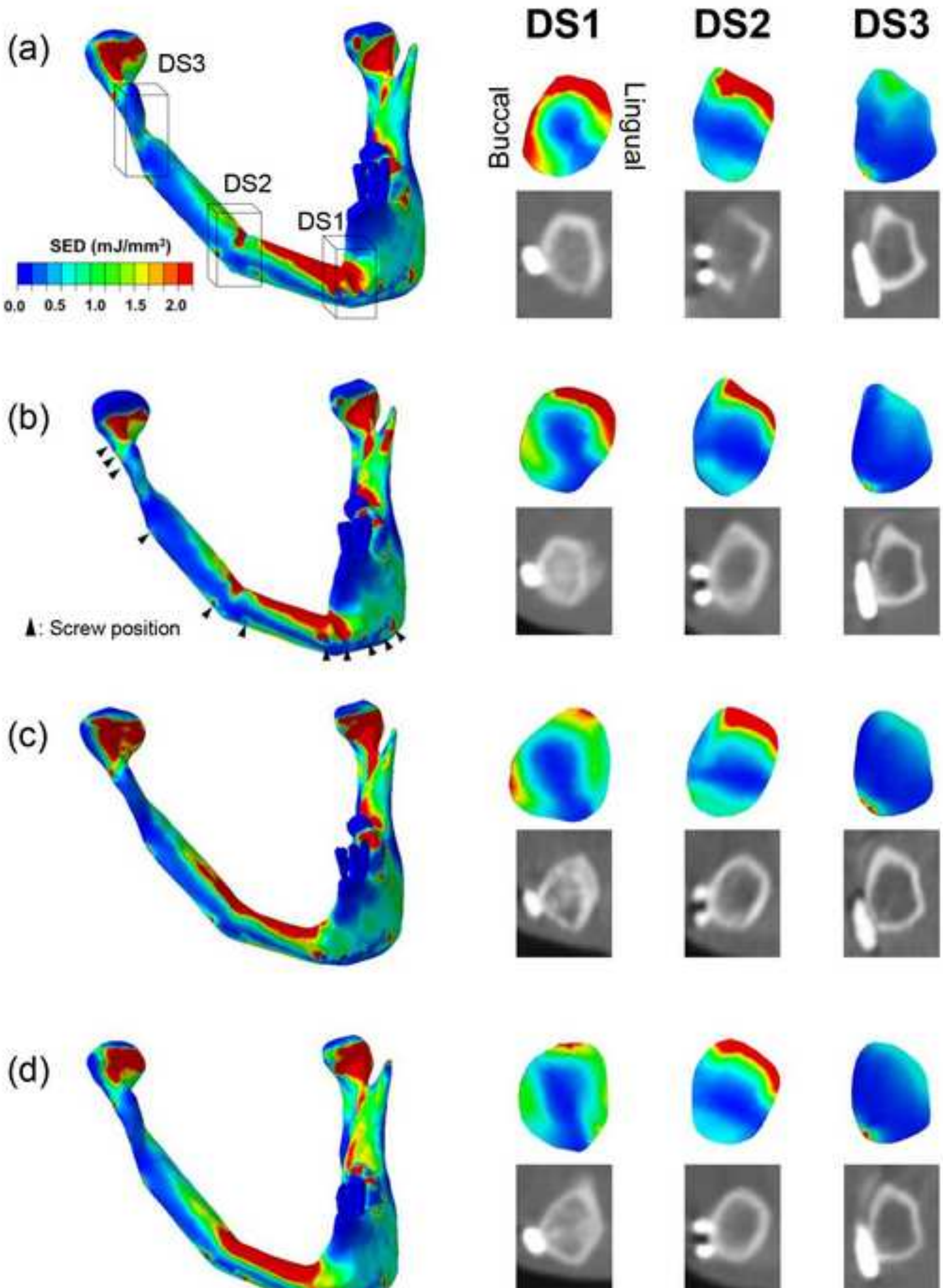

Figure 9
Click here to download high resolution image

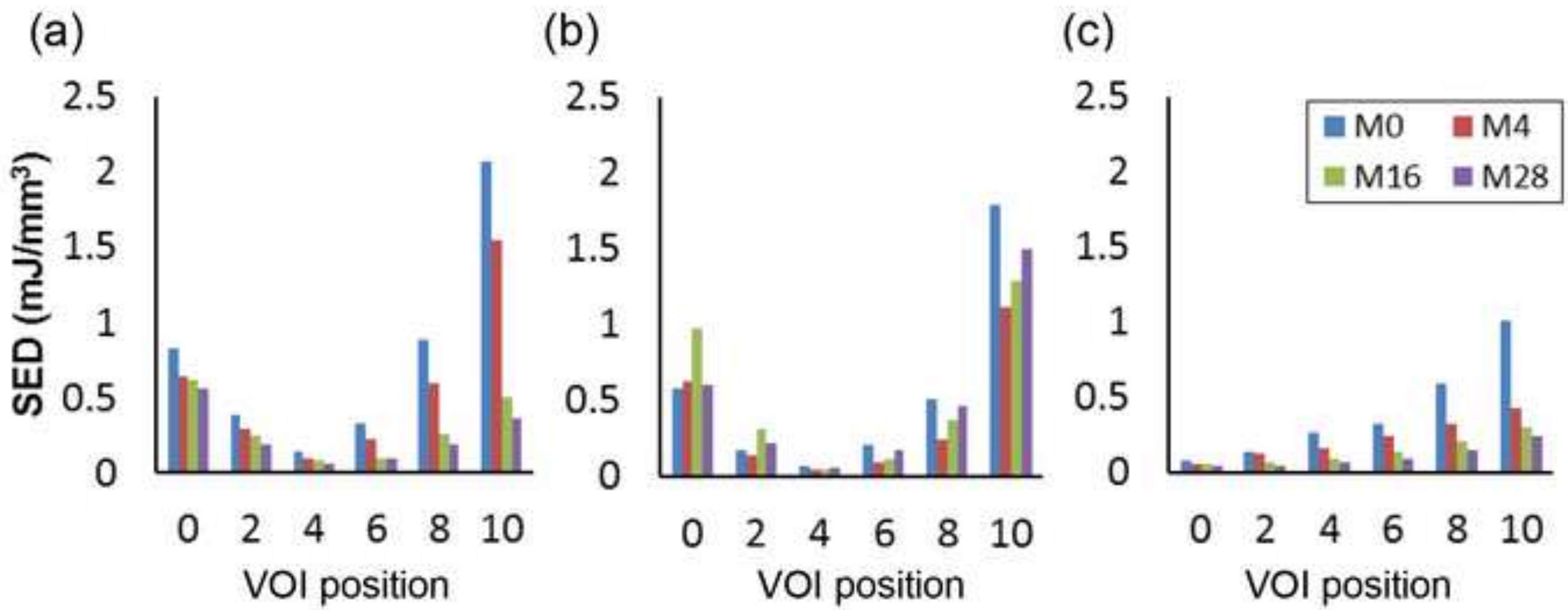

Figure 10

Click here to download high resolution image